

Review

# A Short Review on the Catalytic Activity of Hydrotalcite-Derived Materials for Dry Reforming of Methane

Radosław Dębek<sup>1,2</sup>, Monika Motak<sup>1</sup>, Teresa Grzybek<sup>1</sup>, Maria Elena Galvez<sup>2</sup> and Patrick Da Costa<sup>2,\*</sup>

<sup>1</sup> Faculty of Energy and Fuels, AGH University of Science and Technology, 30 A.Mickiewicza Av., 30-059 Kraków, Poland; debek@agh.edu.pl (R.D.); motakm@agh.edu.pl (M.M.); grzybek@agh.edu.pl (T.G.)

<sup>2</sup> Institut Jean Le Rond d'Alembert, Sorbonne Universités, UPMC, Univ. Paris 6, CNRS, UMR 7190, 2 Place de la Gare de Ceinture, 78210 Saint-Cyr-L'Ecole, France; elena.gavez\_parruca@upmc.fr

\* Correspondence: patrick.da\_costa@upmc.fr; Tel.: +33-1-30-85-48-62

Academic Editor: Simon Penner

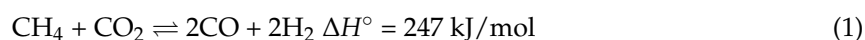
Received: 29 October 2016; Accepted: 12 January 2017; Published: 18 January 2017

**Abstract:** Nickel-containing hydrotalcite-derived materials have been recently proposed as promising materials for methane dry reforming (DRM). Based on a literature review and on the experience of the authors, this review focuses on presenting past and recent achievements on increasing activity and stability of hydrotalcite-based materials for DRM. The use of different NiMgAl and NiAl hydrotalcite (HT) precursors, various methods for nickel introduction into HT structure, calcination conditions and promoters are discussed. HT-derived materials containing nickel generally exhibit high activity in DRM; however, the problem of preventing catalyst deactivation by coking, especially below 700 °C, is still an open question. The proposed solutions in the literature include: catalyst regeneration either in oxygen atmosphere or via hydrogasification; or application of various promoters, such as Zr, Ce or La, which was proven to enhance catalytic stability.

**Keywords:** hydrotalcites; layered double hydroxides; dry reforming of methane; carbon dioxide; nickel

## 1. Introduction

Our worldwide natural gas consumption increases yearly, i.e., in 2014, 12.9 Gtoe were consumed, which is 22.5% higher with the respect to the year 2004. Only in the last year, an increase of 1% in natural gas consumption has been observed [1]. This trend is predicted to develop even faster, since natural gas is the cheapest fossil fuel and possess the highest H/C ratio, contributing to lower CO<sub>2</sub> emissions with respect to other fossil fuels [2]. Nevertheless, CO<sub>2</sub> is still emitted in the energetic utilization of natural gas, e.g., 6.9 Gt of CO<sub>2</sub> were emitted only in 2013, accounting for ca. 22% of total CO<sub>2</sub> emissions [3]. Natural gas and carbon dioxide are therefore closely connected. Finding an appropriate solution to ease the environmental impact of these two gases is crucial for sustainable development in view of a low-carbon dioxide economy, and stays in line with international agreements and policies [4–7]. One of the routes considering the simultaneous energetic valorization of methane and CO<sub>2</sub> is dry reforming of methane (DRM, Equation (1)).



The first investigations concerning the transformation of CO<sub>2</sub> and CH<sub>4</sub> into synthesis gas were reported in 1888. The process was further studied by Fischer and Tropsch in 1928 [8]. Although DRM is not quite a new concept, the dry reforming reaction has again gained considerable attention

in our days, due to the possibility of utilizing two greenhouse gases for the production of a very valuable mixture of  $H_2$  and  $CO$ —a building block for the production of synthetic fuels and chemicals. Moreover, DRM can be used as a way of valorizing natural gas fields containing high amounts of  $CO_2$ , whose extraction is currently economically unprofitable. The concentration of  $CO_2$  in such gas fields can vary from a few percent up to even 70%, as reported for a natural gas field in Indonesia [9]. The studies carried out by Suhartanto et al. [9] confirmed the feasibility of using DRM technology for the energetic valorization of this field, which contains ca. 1320 billion cubic meters of gaseous hydrocarbons. Another possibility is the use of dry reforming in exothermic-endothermic reaction cycle systems for transport and storage of energy using the waste heat from renewables or nuclear energy to power endothermic reactions [10–12], as depicted in Figure 1.

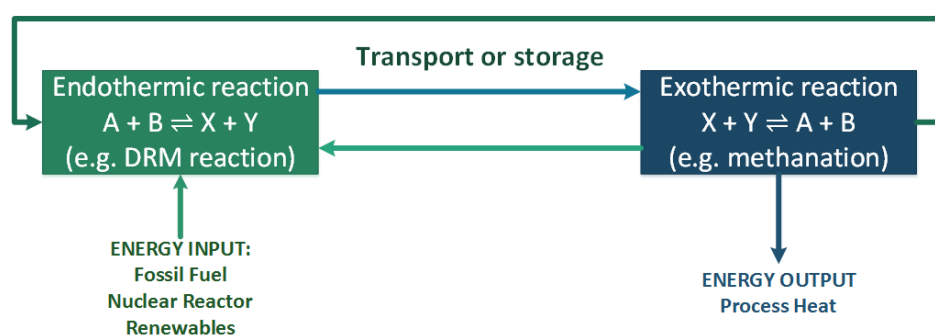


**Figure 1.** Chemical energy storage concept, using heat from renewables or nuclear and dry reforming of methane (DRM) and methanation as energy carriers.

The industrial applications of dry reforming are thus far limited to a combination of steam and dry reforming reactions. The addition of  $CO_2$  into the feed allows a more accurate control of product distribution, i.e., generally resulting in lower  $H_2/CO$  molar ratios. Depending on their application, the different processes differ in operating parameters and feed composition (e.g., SPARG–Sulfur Passivated Reforming or CALCOR– $CO$  through  $CO_2$  Reforming processes) [13–17]. Their main goal is, however, to adjust syngas quality to the needs of its subsequent use, and not the valorization of  $CO_2$  itself. The particular conditions needed for DRM, are a direct consequence of its thermodynamic and kinetic barriers and hinder its practical industrial application. The commercialization of DRM process for syngas production and  $CO_2$  valorization is yet dependent on the offer of a new active and stable catalyst.

During the last few decades, great efforts have been undertaken to develop highly active and stable DRM catalysts. The deactivation of DRM catalysts is mainly caused by: (i) the formation of catalytic coke, which may result in the blockage of pores and active sites; (ii) sintering of active materials, since DRM is carried out at a rather high temperature; and/or (iii) oxidation of metallic active sites. The use of different types of materials as catalyst supports, promoters and preparation methods can lead to overcoming these problems.

In general, transition metals belonging to 8, 9 and 10 groups of the periodic table are active materials for a DRM reaction. Despite the better performance of noble-metal-based catalysts, most of the reported research currently focuses on nickel-based systems, since Ni is much cheaper and more available [18]. In comparison to other non-noble metals such as Fe or Co, nickel-based catalysts are less prone to coking [19]. The research on Ni-based catalysts is currently dedicated mainly to increasing their stability. The high endothermicity of dry reforming of methane requires high temperatures (800–1000 °C). This unavoidably leads to the sintering of nickel particles, since its Tamman temperature is equal to 600 °C [20]. Moreover, deactivation is substantially accelerated as a consequence of carbon deposition, since carbon-forming reactions are thermodynamically favoured in the same temperature window and proceed more easily on large nickel crystallites [21]. Several

approaches have been therefore proposed in order to increase the stability of Ni-based catalysts [22], such as:

- (i) Employing an appropriate preparation method in order to control Ni crystal size and thus inhibit coke growth.
- (ii) Using metal oxides with strong Lewis basicity as supports or promoters, since basic sites enhance CO<sub>2</sub> adsorption. Metal oxides can promote the oxidation of carbon deposits (i.e. via the reverse Boudouard reaction), but, on the other hand, the supports exhibiting Lewis acidity enhance formation of coke deposits.
- (iii) Addition of a second metal, i.e., a noble metal, which may enhance the transport of hydrogen and/or oxygen between active sites and support by spillover, and can influence the mechanism of coke formation. Addition of promoters, such as Ce, Zr or La, in the aim of modifying the selectivity of the DRM process and/or enhancing the gasification of the carbon deposits.
- (iv) Sulphur passivation of Ni catalysts, which blocks the step edge sites where coke build-up is initiated.
- (v) Changing reaction conditions by the addition of oxidizing agents, such as water or oxygen, which can help oxidize carbon deposits.

Different supports have been considered in the preparation of Nickel-based catalysts for DRM, such as single oxides (Al<sub>2</sub>O<sub>3</sub> [23,24], MgO [25,26], CeO<sub>2</sub> [27], ZrO<sub>2</sub> [28], SiO<sub>2</sub> [20,29]); ordered mesoporous silicas (SBA-15 [30], La<sub>2</sub>O<sub>3</sub> [31], TiO<sub>2</sub> [32]), mixed oxides (MgO-Al<sub>2</sub>O<sub>3</sub> [33–35], CeO<sub>2</sub>-ZrO<sub>2</sub> [36], CeO<sub>2</sub>-Al<sub>2</sub>O<sub>3</sub> [37]); zeolites (zeolite Y, zeolite A, zeolite X, ZSM-5) [38]; clays (clinoptolite [39], diatomite [40], vermiculite [41], montmorillonite [42]); and carbon-based materials (carbon nanotubes, activated carbon) [43].

Alumina is one of the most commonly studied supports for nickel catalysts [18,21]. It is relatively cheap and offers high specific surface area, basic character and its  $\alpha$ -Al<sub>2</sub>O<sub>3</sub> phase possesses high thermal stability. However, the catalytic properties of Ni/Al<sub>2</sub>O<sub>3</sub> catalyst in DRM reaction and its resistance to carbon formation depend on the catalyst structure, composition, calcination conditions and preparation method.

Beccera et al. [23] studied the influence of calcination temperature on the activity of impregnated Ni/Al<sub>2</sub>O<sub>3</sub> catalysts. With increase of calcination temperature, higher amounts of NiAl<sub>2</sub>O<sub>4</sub> spinel phase were formed, which suppressed catalytic activity at low temperatures (below 700 °C). At the same time, the formation of spinel phase increased catalyst resistance to coke formation. As explained by Hu et al. [21] this was the result of strengthening of the Ni-O bond in NiAl<sub>2</sub>O<sub>4</sub> with respect to NiO crystal, thus increasing the difficulty of Ni<sup>2+</sup> reduction to Ni<sup>0</sup>, and resulting in the formation of smaller nickel crystallites on the surface. Similar results were reported by Chen and Ren [44]. Bhattacharyya and Chang [45] also reported that NiAl<sub>2</sub>O<sub>4</sub> catalysts prepared through co-precipitation exhibited higher activity and much more stable performance than Ni/Al<sub>2</sub>O<sub>3</sub> prepared by physically mixing of NiO and  $\alpha$ -Al<sub>2</sub>O<sub>3</sub> powders. They claimed that this was due to the formation of a crystalline alpha-alumina phase in the Ni/Al<sub>2</sub>O<sub>3</sub> catalyst. Kim et al. [24] compared the catalytic performance of Ni/ $\gamma$ -Al<sub>2</sub>O<sub>3</sub> and Ni supported on alumina aerogel prepared by a sol-gel method. The preparation method influenced the morphology and size of metal particles distributed on catalyst surface. The catalyst prepared using the alumina aerogel exhibited very high specific surface area, high porosity and narrow distribution of nickel particle size. The impregnation of  $\gamma$ -Al<sub>2</sub>O<sub>3</sub> with the Ni precursor led to irregularly distributed and larger-sized Ni particles. All these facts strongly influenced the catalytic performance of these materials in DRM. Ni supported on alumina aerogel was stable up to 30 h time-on-stream (TOS) and its activity was comparable to a reference 5 wt % Ru/Al<sub>2</sub>O<sub>3</sub> catalyst. On the other hand, the catalyst prepared through impregnation lost its catalytic activity during the first 4–5 h TOS, due to the formation of carbon deposits. According to the authors, the minimal size of nickel crystallites needed for the formation of whisker-type carbon deposits was 7 nm, and thus coking was unavoidable for the Ni/Al<sub>2</sub>O<sub>3</sub> catalyst prepared by the impregnation method, exhibiting bigger and less dispersed

particles. Additionally, due to the weak metal-support interactions, sintering of active phase occurred during the DRM reaction for such catalysts. A different approach was applied by Baktash et al. [46], who prepared the “inverse catalyst.” Aiming at stabilizing the structure and inhibiting sintering of active Ni crystallites, they coated a NiO nanopowder with a thin layer (around few nm) of porous alumina via an atomic layer deposition technique. This NiO powder covered with alumina layers showed stable CH<sub>4</sub> conversion of ca. 80% at 800 °C for up to 12 h TOS. The catalytic activity decreased with increasing alumina layer thickness. Additionally, alumina coating prevented the sintering of active phase leading to decreased coking with respect to the uncoated catalyst. Thus, in the case of alumina-supported catalysts, the type of alumina used and the preparation method can considerably influence the catalytic behaviour of the resulting material, its activity, selectivity and durability in DRM. Moreover, the amount of Ni loaded further determined this interaction and the catalytic performance of these materials. Furthermore, calcination and pre-treatment conditions must be taken into account, not only in the case of alumina-supported catalysts.

Magnesia is another widely studied support for DRM nickel-based catalysts. The high Lewis basicity of MgO has a beneficial effect, since CO<sub>2</sub> adsorption is enhanced on basic supports. Another advantage of using MgO as a support for the preparation of DRM catalysts arises from the possibility of forming a NiO-MgO solid solution at any molar ratio due to the similar anion radii of Mg and Ni cations (Mg<sup>2+</sup> 0.065 nm, Ni<sup>2+</sup> 0.072 nm [26]) and the particular lattice parameters of this mixed oxide structure. The formation of this mixed oxide phase results in increased metal-support interaction, and thus prevents catalyst deactivation via sintering.

The effect of nickel loading on (111) magnesia nano-sheets was studied by Lin et al. [25]. The stability and activity reported were closely related to Ni loading. The catalytic activity in DRM increased with Ni loading up to 10 wt % and then decreased with a further increase in Ni content. The stability for the catalyst containing the highest amount of Ni, i.e., 50 wt %, was very poor. Similar results were reported by Zanganeh et al. [47,48]. In both studies, the best performance was registered for 10 wt % Ni/MgO catalysts, which was attributed to the higher basicity of the studied materials, together with the formation of small nickel crystallites leading to stronger metal-support interaction. It must be mentioned, however, that in both studies the most active catalysts still exhibited the presence of carbon deposits after reaction. The catalysts with the lowest nickel loading (2 wt %) showed decreased CH<sub>4</sub> and CO<sub>2</sub> conversions, which was ascribed to the sintering of the Ni phase or to the oxidation of Ni species. At the same time, insignificant amounts of coke were present on the surface of the spent catalysts. Jafarbegloo et al. [26] also stated that a MgO-supported catalyst loaded with 10 wt % Ni and prepared via one-pot sol-gel/evaporation method exhibited enhanced catalytic performance with respect to other catalysts loaded with higher or smaller amounts of Ni. The results presented in ref. [25,26,47,48] evince that CO<sub>2</sub> conversions were higher than CH<sub>4</sub> conversions at every stage within the whole temperature range considered i.e., 600–850 °C, pointing to the occurrence of the reverse water-gas shift (RWGS) reaction in the presence of MgO-supported catalysts. This in turn results in a decrease in the H<sub>2</sub>/CO molar ratio in the products of the DRM reaction. However, in the experiments carried out by Jafarbegloo et al. [26], an excess of H<sub>2</sub> production was observed, clearly indicating that the method of catalyst preparation still influences the occurrence of side reaction and thus the distribution of the obtained products. MgO is therefore a prospective support for the preparation of Ni-based catalysts for DRM. However, special attention must be paid to Ni loading, and to the method chosen for Ni incorporation, since, together with calcination and pre-treatment conditions, these facts can influence the final Ni crystal size, the interaction of this Ni phase with the MgO support, i.e., the formation of a mixed NiO-MgO phase, and thus the final basicity of the catalysts, resulting in very different catalytic performances.

The beneficial effects of magnesia (enhanced chemisorption of CO<sub>2</sub>) and alumina (enhanced thermal stability, high specific surface area) can be combined in mixed MgO-Al<sub>2</sub>O<sub>3</sub> supports. It has been reported that the addition of MgO into a Ni/Al<sub>2</sub>O<sub>3</sub> catalyst resulted in increased basicity [33,35], specific surface area and total pore volume [33], due to the formation of the MgAl<sub>2</sub>O<sub>4</sub> spinel phase.

The catalytic activity of Ni supported on mixed magnesia alumina depends on the support preparation method, reaction conditions and on the pre-treatment of the catalyst before DRM reaction. Min et al. [33] compared the performance of two catalysts respectively synthesized via a sol-gel and a co-precipitation method. Both catalysts showed acceptably high conversions of  $\text{CH}_4$  and  $\text{CO}_2$  and were stable for to 40 h TOS. Although the catalysts did not differ in activity, the characterization of catalyst after reaction proved the presence of Ni crystallites of larger size in the co-precipitated catalyst vis-à-vis the catalyst prepared through the sol-gel method, clearly pointing to higher deactivation extent due to Ni sintering. Therefore, as sintering proceeded, the subsequent increase in Ni crystal size resulted in a lower resistance to coke formation for the co-precipitated catalyst. The authors examined also the effect of Mg/Al molar ratio in the mixed  $\text{MgO-Al}_2\text{O}_3$  support. The catalysts prepared using intermediate MgO amounts exhibited the highest activity. On the contrary, the studies carried out by Alipour et al. [34] and Xu et al. [35] demonstrated that only a small addition of MgO (up to 5 wt %) to Ni/ $\text{Al}_2\text{O}_3$  enhanced its stability and activity. The influence of the Mg/Al molar ratio on these mixed oxide supports, in addition to catalytic activity and selectivity, remains unclear, probably as a consequence of the simultaneous influence of other important parameters, such as Ni loading, preparation method or the conditions chosen for calcination and pre-treatment.

The preparation of mixed Mg(Al)O phases as well as of nickel catalysts based on these materials may be also realized by means of the thermal decomposition of hydrotalcite-like mixed layered hydroxides. This kind of catalyst has recently been presented in the literature as very promising for DRM, showing high activity and enhanced stability. The present paper reviews the performance of the various Ni-containing hydrotalcite-derived catalysts in dry reforming of methane, reported thus far in the existing literature. The influence of Ni content, Mg/Al ratio, preparation method and pre-treatment conditions will be carefully compared and evaluated.

## 2. Hydrotalcites

Hydrotalcite is a naturally occurring layered mineral, discovered in Sweden in 1842, of chemical formula:  $\text{Mg}_6\text{Al}_2(\text{OH})_{16}\text{CO}_3 \cdot 4\text{H}_2\text{O}$  [49]. The name hydrotalcite comes from its resemblance with talc ( $\text{Mg}_3\text{Si}_4\text{O}_{10}(\text{OH})_2$ ), and from the high water content of this mineral. Similar to talc, the hydrotalcite mineral can be easily crushed into a white powder. Hydrotalcite occurs in nature in foliated and contorted plates and/or fibrous masses [49]. From a crystallographic point of view, this mixed magnesium and aluminium hydroxycarbonate possesses the trigonal structure of brucite, i.e., magnesium hydroxide  $\text{Mg}(\text{OH})_2$ . Hydrotalcite layers are built of octahedral units in which a divalent or trivalent cation is placed in the center of an octahedron and six  $\text{OH}^-$  groups are placed in the corners of the octahedron (Figure 2). As with brucite, octahedral units are linked by edges, forming in this way parallel layers. Depending on the arrangement of the layers, the hydrotalcite structure may have rhombohedral or hexagonal symmetry, in which the unit cell is built up from three and two hydrotalcite layers, respectively. For both naturally occurring and synthetic hydrotalcites, the rhombohedral symmetry is generally more common [49–52].

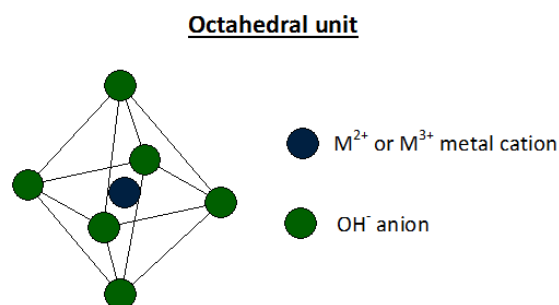


**Figure 2.** The octahedral unit of brucite-like layers in an hydrotalcite structure.



In the hydrotalcite brucite-like layers, a part of the divalent magnesium cations has been isomorphously replaced by trivalent aluminium cations. Such substitution is possibly due to the similar ionic radii of  $Mg^{2+}$  and  $Al^{3+}$ . Thanks to this substitution, the brucite-like layers of hydrotalcite are positively charged. This charge is compensated by carbonate anions present in the interlayer spaces. Water molecules complete the voids in the spaces between the hydrotalcite layers [49–52]. A schematic representation of hydrotalcite structure is presented in Figure 3.

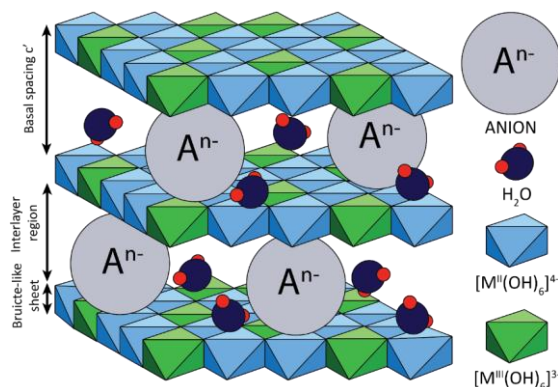
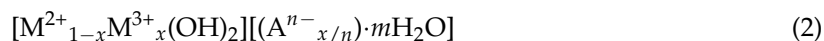


**Figure 3.** Schematic representation of the hydrotalcite structure.

Shortly after the discovery of hydrotalcites, a large number of minerals with different compositions but the same hydrotalcite-like structure were developed. Currently, the name hydrotalcite (hydrotalcite-like compounds—HTs, layered double hydroxides—LDHs) is used to describe a large group of naturally occurring minerals and synthetic materials that possess the typical layered structure of hydrotalcite. The general formula of such compounds can be represented as [50]:



where  $M^{2+}$ ,  $M^{3+}$  are di- and tri-valent cations; A—interlayer anions; and  $x$ —mole fraction of trivalent cations. The part  $[M^{2+}_{1-x}M^{3+}_x(OH)_2]$  describes the composition of brucite-like layers and  $[(A^{n-})_{x/n} \cdot mH_2O]$  describes composition of interlayer spaces.

As reported in the literature and briefly summarized within the introduction of this review, mixed MgO- $Al_2O_3$  materials are promising supports for the preparation of Ni-containing catalysts for DRM. They gather all the advantages of the separated materials guaranteeing, however, a controlled interaction between the Ni phase and its carrier, thus preventing sintering of active material and at the same time avoiding the formation of inactive phases, such as  $NiAl_2O_4$  or NiO-MgO solid solution. Moreover, Ni can be incorporated by different means, i.e., by means of ion exchange in the brucite-like structure through co-precipitation or simply by impregnation. Additionally, through anion exchange or reconstruction it is possible to introduce various promoters into catalytic system.

The methane and  $CO_2$  conversions reported for several Ni-based catalytic systems, including hydrotalcite-derived materials are presented in Figure 4. Note that the direct comparison of catalytic activity is not straightforward, since the values of methane and  $CO_2$  conversions may depend on the specific reaction conditions used in the DRM experiments, and of course on Ni content and on the preparation procedure of each catalyst. However, it is possible to conclude from Figure 4 that the hydrotalcite-derived catalysts are generally placed among the catalytic systems yielding the highest methane and  $CO_2$  conversions of  $CH_4$  in a wide range of reaction temperatures. Moreover, these hydrotalcite-derived catalysts allow acceptable conversions at low reaction temperatures, i.e., at 500 °C. Nickel-containing hydrotalcite-derived catalysts stand therefore as promising catalysts for DRM. This is a consequence of the particular physicochemical features of these materials, such as abundant but moderate strength basicity and controlled Ni crystal size, which will be discussed in detail further

in this review. This is the reason why the research on these types of materials is important, with an increasing amount of contributions being published each year in the last decades, and may contribute to the commercialization of the DRM process.

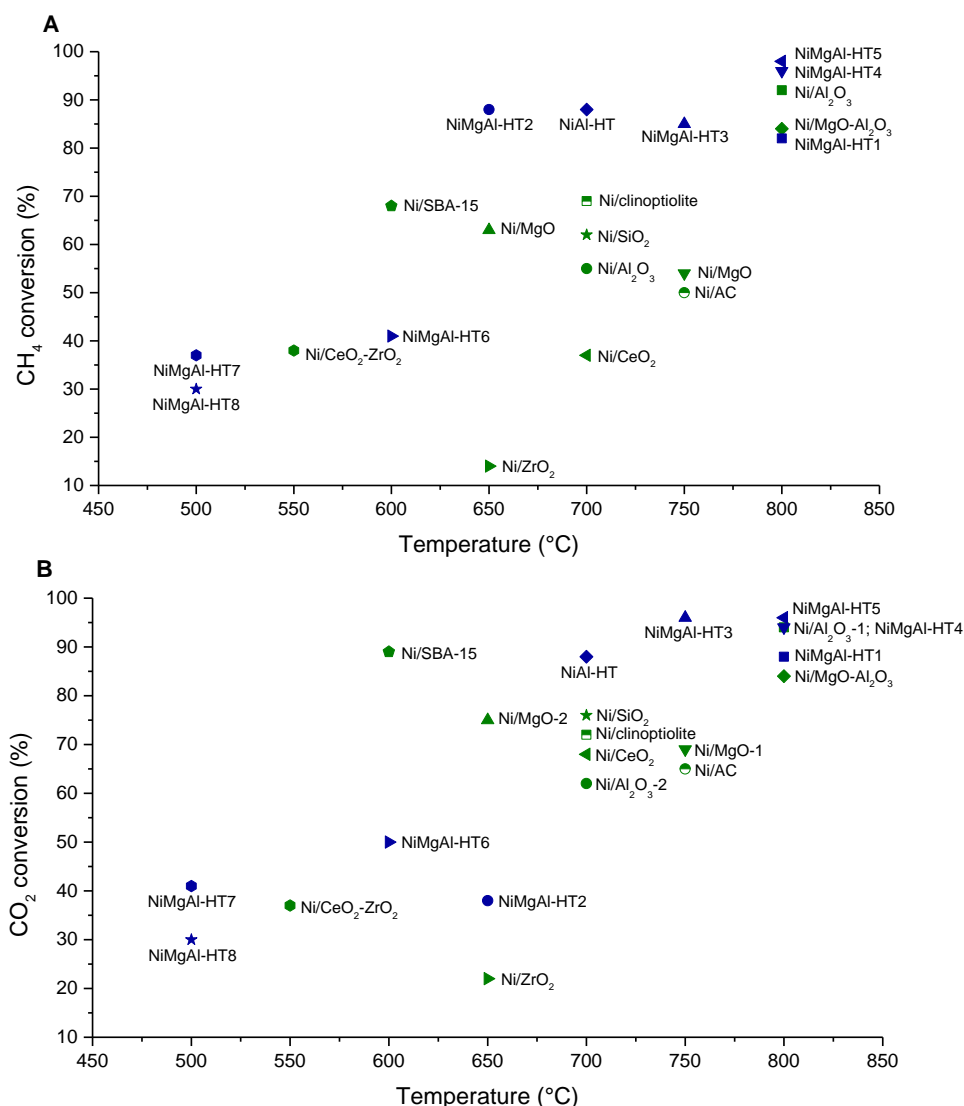


**Figure 4.** Catalytic activity of nickel-based catalysts in dry reforming of methane: (A) CH<sub>4</sub> conversions and (B) CO<sub>2</sub> conversions, as a function of temperature; Green symbols—catalysts Ni/support: Ni/Al<sub>2</sub>O<sub>3</sub>-1 [23], Ni/Al<sub>2</sub>O<sub>3</sub>-2 [24], Ni/MgO-1 [25], Ni/MgO-2 [26], Ni/MgO-Al<sub>2</sub>O<sub>3</sub> [33], Ni/CeO<sub>2</sub> [27], Ni/ZrO<sub>2</sub> [28], Ni/CeO<sub>2</sub>-ZrO<sub>2</sub> [36], Ni/SiO<sub>2</sub> [20,29], Ni/SBA-15 [30], Ni/c clinoptilolite [39], Ni/AC [43]; Blue symbols—hydrotalcite-derived catalysts: NiMgAl-HT1 [53], NiMgAl-HT2 [54], NiMgAl-HT3 [55], NiMgAl-HT4 [56], NiMgAl-HT5 [57], NiMgAl-HT6 [58], NiMgAl-HT7 [59], NiMgAl-HT8 [60], NiAl-HT [61].

### 3. Catalytic Activity of Hydrotalcite-Derived Materials in Dry Reforming of Methane (DRM)

#### 3.1. Ni/Mg/Al and Ni/Al Hydrotalcite-Derived Catalysts

The substitution of a part or all of Mg<sup>2+</sup> cations by Ni<sup>2+</sup> in the Mg/Al-CO<sub>3</sub> hydrotalcite structure results already in a catalytic system that, upon calcination, can be used in dry reforming. Table 1 contains a summary of the different DRM catalysts prepared from Ni/Mg/Al and Ni/Al hydrotalcites.

**Table 1.** Different Ni/Mg/Al and Ni/Al hydrotalcite-derived catalytic materials tested in DRM and reported in the existing literature.

Type of Catalyst	Method of Hydrotalcite Synthesis	Cations in HTs Layers	Ni/Mg or Ni Loading <sup>1</sup>	M <sup>2+</sup> /M <sup>3+</sup>	Calcination Conditions	Reaction Conditions			Conversion <sup>2</sup>		H <sub>2</sub> /CO (-)	Ref.	
						Temp. (°C)	CH <sub>4</sub> /CO <sub>2</sub>	GHSV (h <sup>-1</sup> )	TOS (h)	CH <sub>4</sub> (%)			CO <sub>2</sub> (%)
NiMgAl HTs	Co-precipitation at constant pH	Ni <sup>2+</sup> , Mg <sup>2+</sup> , Al <sup>3+</sup>	1, 0.2	2, 3	nd	815	1.25	720	250	70	52	1.0	[62]
NiMgAl HT	Co-precipitation at constant pH	Ni <sup>2+</sup> , Mg <sup>2+</sup> , Al <sup>3+</sup>	1/6	2.45	700, 900 °C for 14 h	750	1/1	nd	nd	29	50	nd	[63]
NiMgAl HTs	Co-precipitation at constant pH	Ni <sup>2+</sup> , Mg <sup>2+</sup> , Al <sup>3+</sup>	3, 6, 9, 12, 15, 18 <sup>1</sup>	3	800 °C for 5 h	600	1/1 <sup>3</sup>	60,000	25	41	50	0.7	[58]
NiMgAl and NiAl HTs	Co-precipitation at constant pH	Ni <sup>2+</sup> , Mg <sup>2+</sup> , Al <sup>3+</sup>	3, 1, 0.33, 0.18, 0.06	3	550 °C for 4 h in air	550	1/1 <sup>3</sup>	20,000	24	43	40	1.1	[64]
NiAl and NiMgAl HTs	Co-precipitation at constant pH	Ni <sup>2+</sup> , Al <sup>3+</sup>	-	2	800 °C for 6 h in air	750	1/1 <sup>3</sup>	3 × 10 <sup>5</sup>	8	68	90	0.7	[65]
NiMgAl HTs	Co-precipitation at constant pH	Ni <sup>2+</sup> , Mg <sup>2+</sup> , Al <sup>3+</sup>	0.5, 1, 2, 5	0.4, 0.9, 2	400, 600, 800 °C for 6 h in air	650	1/2 <sup>3</sup>	45,000 <sup>4</sup>	nd	83	38	1.2	[54]
NiAl HT	Co-precipitation at constant pH	Ni <sup>2+</sup> , Al <sup>3+</sup>	63 <sup>1</sup>	4	550 °C for 4 h in air	550	2/1 <sup>3</sup>	20,000	4	48	54	2.6	[66]
NiMgAl HT	Co-precipitation at constant pH	Ni <sup>2+</sup> , Mg <sup>2+</sup> , Al <sup>3+</sup>	2.94	2	350, 600, 800, 1000 °C	900	32/40 <sup>3</sup>	nd	10	74	nd	nd	[67,68]
NiMgAl HTs	Co-precipitation at constant pH	Ni <sup>2+</sup> , Mg <sup>2+</sup> , Al <sup>3+</sup>	1/5, 1/3, 1	6, 4, 2, 2/3, 2/5	500 °C for 10 h in air	800	1/1	80,000	30	82	88	nd	[53]
NiAl HTs	Co-precipitation at constant pH	Ni <sup>2+</sup> , Al <sup>3+</sup>	-	2, 3, 5, 8, 10	300, 400, 500, 600, 700, 800 °C for 6 h	700	1/1 <sup>3</sup>	nd	10	88	88	1.0	[61]
NiAl HT	Co-precipitation at constant pH	Ni <sup>2+</sup> , Al <sup>3+</sup>	44 <sup>1</sup>	2	450 °C for 4 h	700	1/1 <sup>3</sup>	nd	30	94	94	0.9	[69]
NiMgAl HTs	Co-precipitation at constant pH	Ni <sup>2+</sup> , Mg <sup>2+</sup> , Al <sup>3+</sup>	1, 5, 25, 50 <sup>4</sup>	2	600 °C for 3 h in air	900	32/40 <sup>3</sup>	nd	10	67	nd	0.8	[70]

<sup>1</sup> weight % of Ni loading; <sup>2</sup> results obtained for the best catalyst; <sup>3</sup> gases were diluted with inert gas; <sup>4</sup> mol % of Ni loaded; nd—no data. Note: Fixed-bed laboratory-scale reactor, except when noted within the text.



The work of Bhattacharyya et al. [62] contains most probably the earliest report on hydrotalcite-derived Ni/Al and Ni/Mg/Al mixed oxides for combined dry/steam reforming. They furthermore compared the catalytic activity of these hydrotalcite-derived materials to commercial NiO-supported catalysts, proving that the use of both Ni/Al and Ni/Mg/Al catalysts resulted in very similar yields and conversions than those obtained in the presence of the commercial catalyst. Moreover, the hydrotalcite-derived catalysts turned out to be more active under more severe reaction conditions (higher gas hourly space velocity (GHSV), and lower H<sub>2</sub>O/CH<sub>4</sub> feed gas composition) and more resistant to coke formation. No further characterization data were nevertheless provided. Several researchers therefore continued the research on these promising materials. Basile et al. [63] prepared Ni/Mg/Al hydrotalcite-derived catalysts having Ni/Mg molar ratios around 1/6. These materials were tested in DRM at very low contact times. They showed very higher activity towards CO<sub>2</sub> and the formation of excess CO in the products of reaction, pointing to the simultaneous occurrence of reverse water gas shift reaction. These results are in good agreement with those presented by other authors [58,64,65] testing HT-derived materials with low nickel content. On the contrary, the materials with high content of Ni in brucite-like layers were reported to promote CH<sub>4</sub> decomposition [54,66–68]. Therefore, the catalytic properties of hydrotalcite-derived materials (activity, stability, promotion of side reactions) are dependent on the materials composition i.e., nickel content, Ni/Mg and Mg/Al molar ratio. This will be discussed in the next subchapter. The temperature and duration of the calcination process has been as well considered, as reflected in Table 1. The temperature, duration and gas composition chosen for the reduction pre-treatment of the catalysts prior to DRM reaction is another important parameter strongly determining their activity. Once the periclase structure is formed, high reduction temperatures are generally needed, i.e., higher than 850 °C, in order to reduce the Ni present in hydrotalcite-derived materials. However, no detailed information can be found regarding the influence of reduction conditions. The size of Ni crystals may vary as a consequence of their sintering at high temperatures. Further research may be needed in order to assess this important point.

### 3.1.1. Effect of Mg/Al, Ni/Mg and Ni/Al Molar Ratios

The influence of Mg/Al molar ratio in Ni/Mg/Al hydrotalcites was first examined by Zhu et al. [53]. These authors considered the variation of the Mg/Al molar ratio from 1/5 to 5. The results of catalytic tests showed that the performance of hydrotalcite-derived materials was dependent on the Mg/Al molar ratio, i.e., their activity increased with increasing Mg/Al ratios, pointing to a strong influence of the presence of MgO. Moreover, the catalyst containing the highest magnesium amount exhibited also the highest resistance to coke formation. However, it is important to remark that high Mg/Al ratios also resulted in the formation of a segregated Mg<sub>5</sub>(CO<sub>3</sub>)<sub>4</sub>(OH)<sub>2</sub>·3H<sub>2</sub>O phase. Thus, the catalytic activity of the catalyst prepared using the highest Mg/Al ratio may have been affected by the presence of isolated MgO.

With respect to the influence of Ni loading and/or Ni/Al ratio, Touahra et al. [61] prepared hydrotalcite-derived Ni/Al mixed oxides using different Ni/Al molar ratios (2, 3, 5, 8, 10), which were subsequently tested in DRM within the temperature range of 400–700 °C. They observed an important influence of the calcination temperature, since NiAl<sub>2</sub>O<sub>4</sub> spinel phase was detected in the catalysts calcined at 800 °C, this fact being, according to the authors, the main reason for the higher stability of these materials in DRM. Moreover, the catalyst prepared using a Ni/Al ratio equal to 2 was showing the best overall catalytic performance. The work described the influence of Ni/Al molar ratio in terms of the final Ni particle size, which affected as well the stability of the material. Therefore, small Ni particles, i.e., around 6 nm in size, are preferred. Let us note here that these catalysts were all pre-treated in pure H<sub>2</sub> at 750 °C for 1 h. This work was continued by Abdelsadek et al. [69] who tested the activity and stability of Ni/Al = 2 hydrotalcite-derived materials in DRM for ca. 40 h, followed by an in situ regeneration of catalyst by means of the hydrogasification of carbon deposits. These catalysts were pre-treated at 650 °C in pure H<sub>2</sub> for 1 h, thus at a lower temperature than the catalysts tested by Touahra and co-workers. The regeneration of the catalysts through hydrogasification resulted in

an increase in DRM activity upon each cycle. The authors attributed this increase in activity to the formation a C-alpha type of carbon deposits upon DRM, which may still result in partial pore blockage but do not irreversibly poison the Ni active sites.

Lin et al. [58] studied the influence of nickel loading within the range of 3–18 wt % in Ni/Mg/Al hydrotalcite-derived catalysts for DRM. The authors found that both CH<sub>4</sub> and CO<sub>2</sub> conversions increased with increasing Ni loading. However, the influence of side reactions, namely CH<sub>4</sub> decomposition and CO disproportionation, was more evident at low temperatures for the catalysts prepared using high nickel content. The 30 h-isothermal experiments, carried out at 600 and 750 °C, showed that the stability of the catalysts was dependent on both reaction temperature and nickel content. At 750 °C, the stability of the catalysts improved with increasing nickel content. The opposite trend was observed at 600 °C. In fact, coke deposition on the catalysts tested at 600 °C increased with Ni loading. Increased Ni contents favored the sintering of Ni particles, and thus the presence of bigger Ni particles resulted in the promotion of carbon-forming reactions. At 750 °C, the amount of coke deposited decreased with increasing Ni content. The authors claimed that different types of carbon structures could be formed as a function of reaction temperature. The formation of encapsulating carbon, i.e., thick graphitic layers growing on the surface of Ni particles, was considered to be responsible for carbon deactivation.

Perez-Lopez et al. [54] studied the effect of the composition and the calcination temperature in the preparation of Ni/Mg/Al hydrotalcite-derived catalysts, using different M<sup>2+</sup>/M<sup>3+</sup> and Ni/Mg molar ratios. They observed that the catalytic performance of Ni/Mg/Al hydrotalcites was mostly affected by the M<sup>2+</sup>/M<sup>3+</sup> molar ratio rather than by the Ni/Mg ratio. The best catalytic performance in DRM was obtained in the presence of the materials prepared using a Ni/Mg ratio between 1–5 and fixed M<sup>2+</sup>/M<sup>3+</sup> ratio around 2, calcined at 600 °C and reduced at 700 °C. For a constant M<sup>2+</sup>/M<sup>3+</sup> ratio, the surface area of the catalysts was found to be independent of Ni content, whereas when the Ni/Mg ratio was kept constant, the surface area decreased drastically with the reduction of the M<sup>2+</sup>/M<sup>3+</sup> ratio, i.e., an increase in Al content resulted in smaller surface areas. Two low M<sup>2+</sup>/M<sup>3+</sup> are not sufficient to develop a spinel mixed oxide structure. However, the catalytic activity was found to be rather independent of surface area and mostly related to Ni crystal size and to Ni/Mg ratios. For a constant Ni/Mg ratio, the catalytic activity decreases as the M<sup>2+</sup>/M<sup>3+</sup> decreased. The selectivity in DRM was found to be influenced by both Ni/Mg and M<sup>2+</sup>/M<sup>3+</sup> ratios. The authors finally claimed that these differences were due to the simultaneous influence of these parameters in the Ni crystal size and in the acid-base properties of the surface. They moreover remarked the influence of the reduction temperature in the activity and selectivity in DRM for this kind of catalysts.

The influence of Ni/Mg molar ratio was further examined by Dudder et al. [70], who tested different catalysts containing 1, 5, 25 and 50 mol % Ni. The activity of these catalysts, evaluated in terms of methane conversion, increased with increasing Ni content, what was attributed to the increasing availability of Ni metal sites. In fact, the best catalytic performance was shown by the 50 mol % Ni-containing catalyst, which was moreover tested for 100 h, evidencing remarkable stability (around 6% activity loss upon 100 h TOS). The type of formed carbon deposits was found to be dependent on both nickel content and reaction temperature. High temperature DRM favored formation of bulk graphitic forms of coke, while carbon nanofibers were formed at lower reaction temperatures. However, Dudder and co-workers claimed that carbon species could be easily removed by O<sub>2</sub> and CO<sub>2</sub> either isothermally or using a temperature ramp, in order to regenerate the original catalytic activity.

Debek et al. [64] have recently considered the influence of Ni/Mg molar ratio in low temperature DRM for hydrotalcite-derived materials. The Ni/Mg molar ratio considered were 3, 1, 0.33, 0.18 and 0.06. A Mg-free NiAl-HT catalyst was also prepared and tested. Similar to the studies carried out by Dudder et al. [70], methane conversion increased with increasing Ni content, whereas CO<sub>2</sub> conversion was found to be maximal for the catalyst containing ca. 20 wt % Ni. Since methane and CO<sub>2</sub> conversion need to be coupled, and equal, in the case of treating equimolar CH<sub>4</sub>/CO<sub>2</sub> mixtures, this catalyst was considered the most effective within this series. Decoupled and far too high methane conversions point

to the simultaneous occurrence of direct methane decomposition, resulting in carbon formation and thus contributing to a faster deactivation of the catalyst, if this is not avoided by regeneration. Direct methane decomposition activity experiments performed on these catalysts further confirmed this fact. Increasing Ni content also resulted in increased Ni crystal size upon reduction and thus promoted this important concomitant reaction. The authors therefore claimed that selectivity could be tailored by means of controlling Ni crystal size and, together with an increased presence of the highest number of basic sites—i.e., especially strong basic sites—can result in inhibited carbon formation through direct methane decomposition.

It can be thus concluded that the Ni content and thus the Ni/Mg ratio, together with Ni/Al and Mg/Al molar ratios, can definitively determine the catalytic activity and selectivity of Ni-containing hydrotalcite-derived catalysts for DRM. DRM activity and selectivity can furthermore affect the stability of the catalysts and thus the different conversions and product distributions related to composition and preparation procedure can be related to the very different behaviors with TOS observed at different reaction temperatures. In general, increasing Ni content results in increased Ni particle or crystal sizes that, particularly at relatively low or moderate temperatures, may result in the promotion of carbon-forming reactions such as direct methane decomposition. Increasing Mg content can be linked to an increase in the overall basicity. Increasing basicity is generally seen as a positive fact, leading to enhanced stability.

### 3.1.2. Effect of the Method of Ni Introduction into Hydrotalcite (HT) Structure

The works discussed in the previous section refer to the incorporation of Ni cations into the brucite-like structure of the hydrotalcite precursors. Nickel can be nevertheless incorporated into hydrotalcite structure by different means, i.e., not only within the brucite-type layers. In fact, the most commonly applied procedure for the preparation of Ni-containing hydrotalcite-derived materials is the co-precipitation of the different cations present in a solution of their corresponding nitrates, yielding a mixed hydroxide structure where Ni has been introduced in its brucite-like layers (e.g., see references cited in the previous section). Other less frequently used methods considered the incorporation of Ni into the interlayer spaces of the hydrotalcite structure, either by the so-called reconstruction method, either through “memory effect” or via ion-exchange. The latter must be carried out using an appropriate hydrotalcite precursor, since carbonate anions are closely packed in the interlayer spaces, and thus it is hard to exchange them by other type of anions [49]. Usually HTs containing monovalent anions between the rhombohedral layers (e.g.,  $\text{NO}_3^-$ ) are applied for ion-exchange modification. The third possibility is to incorporate nickel species on the surface of hydrotalcite crystallites via conventional impregnation or adsorption methods. Table 2 summarizes the hydrotalcite-derived catalysts prepared by means of these different Ni incorporation procedures, recently reported in the existing literature.

Guo et al. [55] used a conventional impregnation method to prepare nickel supported on  $\text{MgAl}_2\text{O}_4$  spinels obtained from Mg/Al hydrotalcite precursors upon their calcination at 800 °C. Their performance was compared to similarly prepared Ni/ $\gamma\text{-Al}_2\text{O}_3$  and Ni/MgO- $\text{Al}_2\text{O}_3$  catalysts. Using the  $\text{MgAl}_2\text{O}_4$  spinel as support resulted in a highly active catalytic system presenting acceptable stability, due to an enhanced dispersion of Ni particles together with the moderate interaction between active phase and support. Other works [33–35], already discussed within the introduction to this review, already evidence the advantages of using  $\text{MgAl}_2\text{O}_4$  spinels as supports in the preparation of Ni-contained catalysts for DRM.

Shishido et al. [71] compared the DRM catalytic activity of a co-precipitated Ni/Mg/Al hydrotalcite-derived catalyst with the performance of 25.1 wt % Ni impregnated  $\text{MgAl}_2\text{O}_4$  (Mg/Al hydrotalcite-derived) catalyst, and other conventional Ni/MgO and Ni/ $\text{Al}_2\text{O}_3$  catalysts. Among them, the co-precipitated Ni/Mg/Al hydrotalcite-derived catalyst exhibited the highest activity at 800 °C, what was explained in terms of the formation of highly dispersed and stable nickel species on the catalyst surface.

**Table 2.** The summary of Ni/Mg/Al hydrotalcite-derived catalysts into which nickel was incorporated via various methods.

Type of Catalyst	Method of Hydrotalcite Synthesis	Cations in HTs Layers	Ni/Mg or Ni Loading <sup>1</sup>	M <sup>2+</sup> /M <sup>3+</sup>	Calcination Conditions	Reaction Conditions				Conversion <sup>2</sup>		H <sub>2</sub> /CO (-)	Ref.
						Temp. (°C)	CH <sub>4</sub> /CO <sub>2</sub>	GHSV (h <sup>-1</sup> )	TOS (h)	CH <sub>4</sub> (%)	CO <sub>2</sub> (%)		
Ni supported on MgAl HTs	Co-precipitation at constant pH	Mg <sup>2+</sup> , Al <sup>3+</sup>	1, 3, 5, 10, 15 <sup>1</sup>	nd	900 °C for 5 h	750	1/1	50,000	10	85	96	0.9	[55]
NiMgAl HTs; Ni supported on MgAl HT	Co-precipitation at constant pH	Ni <sup>2+</sup> , Mg <sup>2+</sup> , Al <sup>3+</sup>	1/2	3	650 and 850 °C for 14 h in air	800	1/1 <sup>3</sup>	54,000	6	94	nd	nd	[71]
	Impregnation of Ni <sup>2+</sup> on MgAl HT	Mg <sup>2+</sup> , Al <sup>3+</sup>	25.1 <sup>1</sup>	3						92	nd	nd	
NiMgAl HTs	Surfactant assisted co-precipitation	Ni <sup>2+</sup> , Mg <sup>2+</sup> , Al <sup>3+</sup>	10 <sup>1</sup>	3	700 °C for 6 h	800	1/1	60,000	35	47	62	nd	[72]
Ni introduced into MgAl HTs	Co-precipitation in [Ni(EDTA)] <sup>2-</sup>	Mg <sup>2+</sup> , Al <sup>3+</sup>	-	3	500 °C for 16 h in air	800	1/1 <sup>3</sup>	nd	150	98	95	1.0	[73]
Ni introduced into MgAl HTs and NiMgAl HTs	Co-precipitation in [Ni(EDTA)] <sup>2-</sup>	Mg <sup>2+</sup> , Al <sup>3+</sup>	1/7	3.5	500 °C for 16 h in air	800	1/1 <sup>3</sup>	nd	6	97	95	1.0	[57]
	Anion exchange	Mg <sup>2+</sup> , Al <sup>3+</sup>	1/11	3.3						97	95	1.0	
	Reconstruction	Mg <sup>2+</sup> , Al <sup>3+</sup>	1/11	3.6						97	94	1.0	
	Co-precipitation	Ni <sup>2+</sup> , Mg <sup>2+</sup> , Al <sup>3+</sup>	1/5	2.5						98	96	1.0	
NiMgAl HTs	Sol-gel method	Ni <sup>2+</sup> , Mg <sup>2+</sup> , Al <sup>3+</sup>	4, 15, 19 <sup>1</sup>	nd	500, 650 °C for 5 h	800	1/1 <sup>3</sup>	2.94 × 10 <sup>-5</sup>	8	96	94	nd	[56]
NiMgAl HTs	Sol-gel method	Ni <sup>2+</sup> , Mg <sup>2+</sup> , Al <sup>3+</sup>		0.25–19	750 °C for 5 h in air	800	1/1 <sup>3</sup>	36,000	40	84	89	nd	[33]
	Co-precipitation at constant pH	Ni <sup>2+</sup> , Mg <sup>2+</sup> , Al <sup>3+</sup>	15 <sup>1</sup>	2						84	89	nd	
NiAl HT and Ni supported on MgAl HT	Co-precipitation at constant pH	Ni <sup>2+</sup> , Al <sup>3+</sup>	63 <sup>1</sup>	4	550 °C for 4 h in air	550 °C	2/1	20,000	1	48	57	2.7	[74]
	Adsorption of [Ni(EDTA)] <sup>2-</sup>	Mg <sup>2+</sup> , Al <sup>3+</sup>	0.8 <sup>1</sup>	3						25	38	1.6	
NiMgAl HTs	Co-precipitation at constant pH	Ni <sup>2+</sup> , Mg <sup>2+</sup> , Al <sup>3+</sup>	10 <sup>1</sup>	1.5–9	800 °C for 3 h	800	1/1	nd	4	86	87	nd	[75]
NiMgAl HTs	Co-precipitation at constant pH	Ni <sup>2+</sup> , Mg <sup>2+</sup> , Al <sup>3+</sup>	10 <sup>1</sup>	3	500–800 °C for 6 h	800	1/1	8000	2000	92	95	0.9	[76]

<sup>1</sup> weight % of Ni loading; <sup>2</sup> results obtained for the best catalyst; <sup>3</sup> gases were diluted with inert gas; <sup>4</sup> mol % of Ni loading; nd—no data.

Tan et al. [72] studied the DRM performance of Ni/Mg/Al mixed oxides prepared from hydrotalcites, which were synthesized via a surfactant-assisted co-precipitation method. The authors used 3 different surfactants at the co-precipitation stage, in order to modify the properties of the resulting material, i.e., their texture, reducibility, structure and nickel distribution on the catalysts surface. The DRM catalytic experiments evidenced that the use of the different surfactants significantly affected the catalytic performance of materials. When co-precipitation was carried out in the presence of tetrapropylammonium hydroxide (TPAOH), the resulting material yielded increased CH<sub>4</sub> and CO<sub>2</sub> conversions. The charge properties and coordination abilities toward metal ions of the different surfactants influenced the metal particle size and promoted or restrained the growth of specific crystal planes. In this sense, the authors showed that both catalytic activity and stability were strongly affected by the exposure of Ni(200) crystal plane (identified X-ray diffraction (XRD) and high resolution transmission electron microscopy (HRTEM), i.e., fast Fourier transform (FFT) images). These Ni(200) planes were furthermore formed during reaction at high temperatures upon a slow release of Ni encapsulated within the support, and were assumed to be responsible for the stabilization of the catalytic activity, without providing further details on the reaction mechanism. Nevertheless, all the tested catalysts showed a considerable decrease in their catalytic activity at 800 °C over 40 h-DRM experiments.

Tsyganok et al. [73] proposed a new method of Ni introduction into hydrotalcite structure by co-precipitation of a Mg/Al hydrotalcite in a solution of stable [Ni(EDTA)]<sup>2-</sup> chelates. The so-prepared materials evidenced the presence of nickel-EDTA species in the interlayer spaces of the pristine hydrotalcite structure. An important advantage of this method vis-à-vis the conventional co-precipitation of Ni/Mg/Al hydroxides is that the reduction pre-treatment is not required, still the stabilization of the catalytic systems needed from 30 to 90 min induction time. The catalyst showed stable performance during 150 h DRM tests at 800 °C. Different forms of coke deposits were however found on the surface of the spent catalysts, pointing to the simultaneous occurrence of carbon-forming reactions. However, carbon deposition did not seem to affect the catalytic activity. These materials yielded moreover higher conversion of CO<sub>2</sub> than of methane, pointing to the concomitant occurrence of RWGS reaction and thus influencing the product distribution.

In a subsequent work, Tsyganok et al. [57] compared the DRM catalytic performance of Ni-containing hydrotalcite-derived catalysts prepared following different routes, such as: co-precipitation of Mg<sup>2+</sup> and Al<sup>3+</sup> with pre-synthesized [Ni(EDTA)]<sup>2-</sup> complexes; anion exchange reaction of NO<sub>3</sub><sup>2-</sup> ions in the hydrotalcite interlayer spaces with [Ni(EDTA)]<sup>2-</sup> chelate in aqueous solution; calcination of Mg/Al hydrotalcite at moderate temperature, followed by reconstruction of hydrotalcite layered structure in an aqueous solution of [Ni(EDTA)]<sup>2-</sup>; and traditional co-precipitation of Ni<sup>2+</sup>, Mg<sup>2+</sup> and Al<sup>3+</sup> with CO<sub>3</sub><sup>2-</sup>. In spite of the differences in Ni crystal size, all the catalysts prepared using [Ni(EDTA)]<sup>2-</sup> chelates showed stable performance and high conversions of both CH<sub>4</sub> and CO<sub>2</sub>. The highest amount of deposited carbon was indeed found for the catalyst prepared through traditional co-precipitation. Döbek et al. [74] also studied the effect of nickel introduction into hydrotalcite-based catalytic systems, and compared the performance of Ni/Al mixed oxides with Mg/Al hydrotalcite into which nickel was introduced via the adsorption of [Ni(EDTA)]<sup>2-</sup> complexes. The results showed that both catalysts were active in DRM at 550 °C. However, the material into which nickel was introduced by means of the adsorption of [Ni(EDTA)]<sup>2-</sup> chelates exhibited higher activity per gram of active material, with the respect to the catalysts into which nickel was introduced into the brucite-like layers of the pristine hydrotalcite via the conventional co-precipitation method.

Though conventional impregnation of MgAl<sub>2</sub>O<sub>4</sub> spinels derived from the calcination of Mg/Al hydrotalcites already yields good results in the preparation of Ni-containing hydrotalcite-derived catalysts for DRM, the co-precipitation of Ni/Mg/Al hydroxides can lead as well to an uncomplicated synthesis of highly performing hydrotalcite-derived materials. Other methods, such as the incorporation of Ni species in the form of [Ni(EDTA)]<sup>2-</sup> chelates need to be further explored, since they may offer important advantages, such as bypassing the reduction pre-treatment of the catalyst.



However, the surface of the catalysts and the state of Ni species may change upon TOS, and indeed, relatively long induction periods seem to be needed.

### 3.1.3. Influence of the Air-Calcination Temperature

The thermal stability of hydrotalcite-like materials is an important issue, since the products of their thermal decomposition of layered double hydroxides (LDHs) find application not only in DRM catalysis but also in various branches of industry. Although hydrotalcite-like materials may greatly differ in their composition, they exhibit similar thermal decomposition behaviour [50]. This usually comprises four consequent steps [77]: (i) the removal of water physically adsorbed on the external surfaces of the crystallites (below 100 °C); (ii) the removal of interlayer water (up to 250 °C); (iii) the removal of hydroxyl groups from the layers as water vapour; and (iv) the decomposition of the interlayer anions (up to 500 °C). Steps (iii) and (iv) usually overlap. Thermal treatments up to 500 °C are normally associated with the loss of ca. 40 wt % of the initial weight and have been reported for several hydrotalcite-like materials, which differed in composition [49,77–80]. As a result of this thermal decomposition, the lamellar structure of hydrotalcites collapses and a new phase of periclase-like mixed nano-oxides is obtained, i.e., analogous to the cubic form of MgO where the different oxides appear mixed and exhibit crystal sizes in the order of several nanometers [50].

Water, together with the gaseous products of anion decomposition, are released during the thermal treatment of the hydrotalcite structure, can create channels in brucite-like layers and lead to the formation of additional porosity, mostly within the range of mesopores. Thus, the mixed oxides obtained upon calcination are usually characterized by higher specific surface areas, in comparison to their parental hydrotalcite materials [49]. Upon further heating, the periclase-like structure of the mixed oxides may undergo further structural changes, leading to the formation of a stable spinel phase. This phenomenon is dependent on material composition and usually takes place at high temperatures (above 700 °C). However, e.g., the formation of MgFe<sub>2</sub>O<sub>4</sub> spinel was reported for Mg-Fe-CO<sub>3</sub> hydrotalcite already upon heating at 350 °C [50]. Therefore, selection of appropriate calcination temperature is an important factor that may determine catalytic activity in DRM. A summary of different works considering and discussing the effect of calcination temperature in the DRM performance of hydrotalcite-derived catalysts is presented in Table 3.

**Table 3.** The effect of calcination temperature on hydrotalcite (HT)-derived materials in dry reforming of methane (DRM).

Type of Catalyst/Method <sup>1</sup>	Calcination Conditions <sup>2</sup>	Effect of Calcination Temperature	Ref.
NiAl HT/CP	300, 400, 500, 600, 700 and 800 °C for 6 h	Calcination temperature <500 °C has minimal effect of activity; Increase in calcination temperature resulted in increased activity and stability	[61]
NiMgAl HT/CP	400, 600, 800 °C for 6 h	Calcination temperature had a small influence on the activity and selectivity	[54]
NiMgAl HTsSG	500, 650 °C for 5 h	Moderate calcination temperatures prevent formation of spinel phase. Higher calcination temperature resulted in the increased stability	[56]
NiMgAl HT/CP	500, 600, 700, 800 °C for 6 h	No significant effect of calcination temperature on performance in DRM was observed	[76]
NiMgAl HT/CP	350, 600, 800, 1000 °C	Calcination at 800 and 1000 °C resulted in formation of spinel phase. The optimal calcination temperature was selected to be 600 °C	[67,68]

<sup>1</sup> Method of HT synthesis: CP-co-precipitation; SG-sol-gel method; <sup>2</sup> Calcination in air.



Thouahra et al. [61] examined the influence of the calcination temperature on the performance of Ni/Al catalysts. They concluded that the use of calcination temperatures below 500 °C did not practically affect the catalytic activity. In this way, the catalysts calcined at 300 and 400 °C exhibited very similar values of specific surface area and Ni particle size. On the contrary, calcination temperatures above 500 °C could strongly influence the final catalytic properties of the prepared materials, due to the formation of different spinel phases, which resulted in increased interaction between Ni and Al. A decrease in Ni particle size with increasing calcination temperature was thus observed. The highest stability and activity was recorded by Ni/Al catalyst calcined at 700 °C. The studies carried out by Perez-Lopez et al. [54] evidenced, however, that for Ni/Mg/Al hydrotalcite-derived catalysts, the calcination temperature had a minimal effect on the catalytic activity. Similar results, presented by Li et al. [76], showed that calcination temperature did not significantly affect the catalytic activity of Ni/Mg/Al hydrotalcite-derived catalysts containing 10 wt % Ni. These authors observed, however, that crystal size of the periclase-like phase of mixed oxides increased with increasing calcination temperature. The formation of NiAl<sub>2</sub>O<sub>4</sub> spinel phase was, however, not observed and the catalysts calcined at 600, 700 and 800 °C exhibited very similar performance in DRM at 800 °C. It seems therefore that the presence of Mg inhibited the formation of mixed spinel phases in these materials.

Gonzalez et al. [56] considered the sol-gel preparation of Ni/Mg/Al hydrotalcite-derived mixed oxides with 4, 15 and 19 wt % Ni. They studied the influence of moderate calcination temperatures (500–650 °C) in order to avoid the formation of spinel structures. The resulted materials also promoted side reactions, such as CH<sub>4</sub> decomposition, Boudouard reaction and RWGS. The best catalytic performance was observed for the catalyst containing 19% Ni and calcined at 650 °C. The calcination temperature influenced the amount of carbon formed during reaction, i.e., it decreased with increasing calcination temperature. Mette et al. [67,68] investigated performance of Ni/Mg/Al hydrotalcite-derived catalysts with high Ni loading (55 wt %) calcined and reduced in various conditions. Calcination at 800 and 1000 °C resulted in the formation of spinel phases, inactive in DRM. Authors confirmed that temperature 600 °C is sufficient to obtain an amorphous, fully dehydrated and carbonate-free NiMgAl mixed oxide, whose catalytic activity in DRM might be further tailored by the subsequent modification of reduction temperature. The most active and stable catalysts for DRM at 900 °C was the one prepared via calcination at 600 °C, followed by reduction at 800 °C.

### 3.2. Effect of the Addition of Different Promoters

#### 3.2.1. Ce Promotion

Ceria is well known for its high oxygen storage capacity linked to the redox transformation between Ce<sup>3+</sup> and Ce<sup>4+</sup> [36,81]. Therefore, the application of ceria as a promoter for hydrotalcite-derived catalysts in DRM reaction may be beneficial, due to easier removal of carbon deposits via oxidation by oxygen anions. Moreover, nickel can dissolve in the fluorite structure of CeO<sub>2</sub>. The Ni-O-Ce bond is stronger than Ni-O bond in the NiO crystal, thus leading to increased metal-support interactions in ceria-supported Ni systems, resulting in the formation of small Ni particles. The comparison of different methods of ceria introduction into Ni/Mg/Al hydrotalcite-derived mixed oxides reported in literature is presented in Table 4.

The addition of cerium to Ni/Mg/Al hydrotalcites was widely studied by Daza et al., who investigated the effect of the method for the introduction of cerium [82], Ce loading [59,60,83] and the general hydrotalcite preparation procedure [84]. The authors compared the DRM catalytic performance registered for a non-promoted Ni/Mg/Al catalysts and for Ce-promoted co-precipitated catalysts (containing 5 wt % Ce) prepared through co-precipitation in solutions of Na<sub>2</sub>CO<sub>3</sub>, [Ni(EDTA)]<sup>2-</sup> and [Ce(EDTA)]<sup>-</sup> [82]. In all cases, the ceria-promoted catalysts exhibited higher activity than the non-promoted catalyst. The promoting effect of ceria was attributed to the increase of reducibility of nickel species without observing in all cases a simultaneous reduction in the resulting Ni particle size. The best catalytic performance was observed for the catalyst obtained by conventional co-precipitation

in  $\text{Na}_2\text{CO}_3$ , with average  $\text{CH}_4$  and  $\text{CO}_2$  conversions after 200 h TOS equal to ca. 78% and 87%, respectively. Moreover, it was observed that the catalysts prepared using low Ni content and prepared via co-precipitation in solution of  $[\text{Ni}(\text{EDTA})]^{2-}$  complexes exhibited similar performance to the samples loaded with much higher Ni content. This was attributed to the formation of very small nickel crystallites (smaller than 5 nm), in the presence of Ce and especially for catalysts prepared in the presence of  $[\text{Ni}(\text{EDTA})]^{2-}$  complexes.

**Table 4.** Methods of ceria introduction into Ni/Mg/Al hydrotalcite-derived mixed oxides tested in DRM.

Method of Hydrotalcite Synthesis	Method of Ce Introduction into HT Structure	Ni/Mg	Ce Content (wt %)	Calcination Conditions	Ref.
Co-precipitation in solution of $\text{Na}_2\text{CO}_3$ , $[\text{Ce}(\text{EDTA})]^-$ or $[\text{Ni}(\text{EDTA})]^{2-}$	At co-precipitation stage in form of $\text{Ce}^{3+}$ cations or $[\text{Ce}(\text{EDTA})]^-$	1/2	5	500 °C for 16 h in air	[82]
Co-precipitation at constant pH	Reconstruction method with solution of $[\text{Ce}(\text{EDTA})]^-$	2	0, 1, 3, 5, 10	500 °C for 16 h in air	[83]
Co-precipitation at constant pH	Reconstruction method with solution of $[\text{Ce}(\text{EDTA})]^-$	2	0, 1, 3, 10	500 °C for 16 h in air	[60]
Co-precipitation at constant pH	At co-precipitation stage in form of $\text{Ce}^{3+}$ cations	2	24, 9, 4, 1,5 <sup>1</sup>	500 °C for 16 h in air	[59]
Co-precipitation at constant pH and self-combustion method	Reconstruction method with solution of $[\text{Ce}(\text{EDTA})]^-$	2	3	500 °C for 16 h in air	[84]
Co-precipitation at constant pH	At co-precipitation stage in form of $\text{Ce}^{3+}$ cations and by impregnation	20 <sup>2</sup>	1–10 <sup>1</sup>	500 °C for 4 h	[86]
Co-precipitation at constant pH	Adsorption from the solution of $[\text{Ce}(\text{EDTA})]^-$	0.6 <sup>2</sup>	1.15	550 °C for 4 h	[88]
Co-precipitation at constant pH	Adsorption from the solution of $[\text{Ce}(\text{EDTA})]^-$	1/3	3.7	550 °C for 4 h	[87,89]
Co-precipitation at constant pH	At co-precipitation stage in form of $\text{Ce}^{3+}$ cations	10, 25 <sup>2</sup>	5	650 °C for 5 h	[85]

<sup>1</sup> Al/Ce molar ratio; <sup>2</sup> weight % of Ni, otherwise Ni/Mg ratio refers to the ions.

Daza et al. [83] also studied the influence of Ce content in Ni/Mg/Al hydrotalcite-derived catalysts. Ceria was introduced into hydrotalcite structure by reconstruction method using  $[\text{Ce}(\text{EDTA})]^-$  complexes. The Ce and nominal loading was equal to 0, 1, 3, 5 or 10 wt %. Ce-promoted materials exhibited an increase in total basicity with increasing ceria content, upon their calcination and reduction. Using X-ray photoelectron spectroscopy (XPS), the authors further confirmed the coexistence of  $\text{Ce}_2\text{O}_3$  and  $\text{CeO}_2$  on the catalyst surface. During DRM,  $\text{CO}_2$  can be adsorbed on  $\text{Ce}_2\text{O}_3$  sites, yielding CO and  $\text{CeO}_2$  in a redox cycle. The produced  $\text{CeO}_2$  can further react with deposited carbon, regenerating both  $\text{Ce}_2\text{O}_3$  and  $\text{CO}_2$ . This proposed mechanism may explain the increase in total basicity and the increased stability of Ce-promoted catalysts and is in good agreement with results presented recently by Lino et al. [85]. In general, higher conversions of  $\text{CH}_4$  than  $\text{CO}_2$  were observed for ceria-containing samples, which may be explained by the conversion of methane into light hydrocarbons or simply due to direct methane decomposition. The amount of Ce introduced did not have significant influence on  $\text{CH}_4$  and  $\text{CO}_2$  conversions and  $\text{H}_2/\text{CO}$  molar ratio. However, it influenced the formation of carbon deposits. The smallest amounts of catalytic coke were formed on the samples loaded with small amounts of Ce, between 1–3 wt %. Thus, the authors stated that the optimal nominal amount for Ce promotion was 3 wt % [60]. Similar conclusions were driven in another study of the same authors, where ceria was introduced into the hydrotalcite-derived catalytic system at the co-precipitation [59]. Catalysts prepared using different Al/Ce molar ratios were studied. The reducibility of the catalysts increased with increasing ceria content, i.e., decreasing Al/Ce ratios,

which resulted in the formation of bigger Ni crystallites, and thus had a negative effect on the catalysts' stability. The same authors also compared the performance of Ni/Mg/Al hydrotalcites synthesized via co-precipitation and self-combustion in glycine methods [84]. Mixed oxides obtained through calcination of the resulting hydrotalcites underwent additional reconstruction in presence of a solution of  $[\text{Ce}(\text{EDTA})]^-$  complexes. The catalyst prepared from the self-combusted hydrotalcite showed enhanced performance. Its higher activity was related by the authors to its higher specific surface area, pore volume and total basicity.

Recently, Ce-promoted Ni/Mg/Al hydrotalcite-derived catalysts have been as well considered by Ren et al. [86], who investigated DRM reaction at moderate pressure (0.5 MPa). The results confirmed important anti-coking benefits of ceria addition. However, the effect of Ce promotion depended on the amount and the method of ceria introduction. The Ce-impregnated catalysts were more effective in the formation of coke deposits than the co-precipitated ones, which was associated with the higher content of  $\text{Ce}^{3+}$  on the catalyst surface and to an increased presence of lattice defects in the  $\text{CeO}_2$  present in the former catalysts. These materials were very active in DRM and showed an initial  $\text{CH}_4$  conversion at 750 °C very close to the thermodynamic equilibrium limit. However, carbon deposition was observed over the catalyst surface. The amount of coke deposited, and thus the deactivation of catalyst, increased with increasing of Ce loading. These results are in agreement with those reported by Daza et al. [83], who also reported that high loading of ceria may have a negative effect on catalyst stability, due to the enhanced reducibility of nickel species, leading to the formation of bigger crystallites on the catalyst surface.

Đebek et al. [87] proposed a method of Ce addition into HT structure via adsorption from a solution of  $[\text{Ce}(\text{EDTA})]^-$  complexes. Ce addition resulted in an increased reducibility of the nickel species and in the introduction of new, strong (low coordinated) oxygen species and intermediate (Lewis acid-base pairs) strength basic sites, which increased the  $\text{CO}_2$  adsorption capacity. The DRM activity of these materials consequently increased, especially in terms of  $\text{CO}_2$  conversion. Instead, Ce promotion lowered  $\text{CH}_4$  conversion with respect to unpromoted catalysts, which was attributed to the partial inhibition of direct methane decomposition. These authors concluded that Ce promotion could change selectivity of the process and moreover determine type of carbon deposits, i.e., amorphous or graphitic, formed upon the DRM reaction. In a subsequent work [88], they proved that the effect of ceria promotion is also dependent on the method of Ni introduction. The incorporation of Ni species via adsorption of  $[\text{Ni}(\text{EDTA})]^{2-}$  complexes followed by ceria promotion resulted in increased activity, stability and selectivity and yielded a stoichiometric syngas as reaction product, in comparison to the non-promoted catalyst.

### 3.2.2. Other Promoters

The use of different promoters of NiMgAl hydrotalcite-derived catalysts other than cerium has been reported in the literature of the last few years. Table 5 contains a summary of these published works, the promoter used and the results observed upon their addition to the hydrotalcite-derived catalysts.

Yu et al. [90] investigated the addition of La into Ni/Mg/Al hydrotalcite-derived catalysts. The effect of lanthanum was positive on both catalyst stability and activity, within the temperature range 600–700 °C. La addition increased total basicity and surface Ni content of the catalyst, resulting in a considerable suppression of coking. The best catalytic performance was registered for the sample with a nominal La/Al molar ratio of 0.11, which at 700 °C yielded  $\text{CH}_4$  and  $\text{CO}_2$  conversions equal to 76% and 72%, respectively. A similar positive effect of lanthanum addition, in terms of catalyst stability, was observed by Serrano-Lotina et al. [91,92]. However, a decrease in the catalytic activity with TOS was still observed, assigned to the decrease in Ni crystallinity in the La-promoted catalyst. Liu et al. [93], on the other hand, reported an enhanced catalytic activity towards  $\text{CH}_4$  conversion, which was explained in terms of the increase of Ni particle size and the simultaneous promotion of direct methane decomposition. However, the amounts of carbon deposited on the surface of the

catalysts were lower than expected. Through the formation of oxycarbonate species ( $\text{La}_2\text{O}_2\text{CO}_3$ ), La promotion contributed to the gasification of amorphous carbon deposits. The optimal La content was found to be ca. 4 wt %. The different results obtained upon La promotion of these Ni-containing hydrotalcite-derived catalysts are most probably a result of using different La loads and different La incorporation methods. Moreover, the conditions chosen for the calcination and pre-treatment of these materials surely further determine its catalytic behaviour in DRM.

**Table 5.** Effect of different promoters on the performance of NiMgAl hydrotalcite-derived catalysts for DRM.

Promoter	Catalyst	Promoter Loading (wt %)/Method <sup>1</sup>	Effect of Addition	Ref.
La	NiMgAl-HT	0, 0.04, 0.11, 0.18 <sup>2</sup> /CP	Increased stability and activity	[90]
La	NiMgAl-HT	1.1, 2/CP	Increased stability and decreased activity	[91,92]
La	NiMgAl-HT	0, 1, 2, 4/CP	Increased activity, selectivity and stability	[93]
La Rh	10 wt % Ni impregnated on MgAl-HT	10/IMP 1/IMP	Increased reducibility of Ni; promotes carbon formation	[94]
CeZrO <sub>2</sub>	NiMoMgAl-HT	0, 5, 10, 15, 20/CP	Increased catalyst activity; promotes reducibility of Ni	[95]
Ru	5 wt % Ni supported on MgAl-HT	0.1/RE	Inhibits sintering; increased activity and stability	[96]
Co	NiMgAl and NiCoMgAl-HTs	1, 4 <sup>3</sup> /CP	Increased activity and stability	[97]
Co	NiCoMgAl-HTs	2.76–12.9/CP	nd <sup>4</sup>	[98]
Zr	NiMgAl-HT	3/CP	Decreased reducibility; formation of small Ni crystallites; increased stability	[89]

<sup>1</sup> Preparation methods: IMP—Impregnation; CP—Co-precipitation; RE—reconstruction in the solution of  $[\text{M}^{n+}(\text{EDTA})]^{(4-n)-}$  chelates; <sup>2</sup> nominal La/Al molar ratio; <sup>3</sup> nominal Ni/Co molar ratio; <sup>4</sup> nd—no data, since performance of catalyst was not compared to reference Ni-based sample.

Lucredio et al. [94] studied La and/or Rh addition into Ni supported on MgAl-hydrotalcite. The results showed that the addition of both La and Rh resulted in increased reducibility of nickel species. Thus, more Ni active sites were formed on the catalyst surface. Indeed, the catalyst promoted with both Rh and La showed higher activity in terms of CO<sub>2</sub> conversion. However, a negative effect of promoter addition was observed, as Rh- and La-promoted samples exhibited higher amounts of carbon deposited after 6 h TOS at 750 °C.

The DRM catalytic activity of Ni/Mg/Al hydrotalcite-derived catalysts promoted with Ru was studied by Tsyganok et al. [96]. The addition of small amounts of Ru into the catalyst structure by means of a reconstruction method had a highly positive effect on the catalytic performance. Ru promotion inhibited the sintering of Ni crystallites, thus enhancing the stability of the promoted catalyst. Moreover, the authors showed that a better performance of both catalysts was achieved when hydrotalcite samples were calcined/reduced in situ, and concluded that calcination prior to the reaction may result in sintering of NiO.

Molybdenum has been also used in the preparation of Ni-containing bimetallic hydrotalcite-derived catalysts for DRM. The presence of Mo is thought to stabilize Ni species. Li et al. [95] prepared Ni-Mo/Mg(Al)O hydrotalcite-derived catalysts that they further promoted using Ce and Zr. These catalysts showed poor selectivity and were found to be considerably active in the RWGS reaction at 800 °C. The authors confirmed the formation of a complex support of Ce<sub>0.8</sub>Zr<sub>0.2</sub>-Mg(Al)O, whose presence was beneficial in terms of catalytic activity. They further stated that the cycling of Ce<sup>4+</sup>/Ce<sup>3+</sup> contributes to the oxidation of carbon deposits at temperatures higher than 900 °C, in agreement with

the results about Ce promotion discussed previously in this review. No details are provided, however, regarding the role of Mo in this bimetallic catalyst.

Long et al. [97] investigated the activity of Ni-Co bimetallic hydrotalcite-derived catalysts for DRM. The results showed that the addition of Co in an appropriate amount had a positive effect on the catalytic performance. The catalysts were characterized by X-Ray Diffraction (XRD), X-Ray Photoelectron Spectroscopy (XPS), Transmission Electron Microscopy (TEM) and N<sub>2</sub> adsorption techniques. The sample with Ni/Co molar ratio equal to 4 showed the highest conversions of CO<sub>2</sub> and CH<sub>4</sub> and a stable performance in DRM at 700 °C up to 100h TOS. This was explained by synergetic interactions between Ni and Co, which resulted in the formation of highly dispersed small Ni crystallites. On the contrary, Zhang et al. [98] reported the best performance of Ni-Co hydrotalcite-derived catalysts for Ni/Co molar ratios close to unity. The authors, however, noted that the amount of metals had also an effect on the catalyst performance, and catalysts with low content of Ni (1.83–3.61 wt %) and Co (2.76–4.43 wt %) showed better performance.

As explained before, Li et al. [95] considered the simultaneous use of Ce and Zr as promoters. Dębek et al. [89] also considered the utilization of Ce, Zr and Ce-Zr as promoters of Ni/Mg/Al hydrotalcite-derived catalysts for DRM at low temperatures, i.e., 550 °C. The results obtained in the DRM experiments are summarized in Figure 5. The characterization of the materials evidenced that Ce species were present as a separate phase on the material surface, while Zr<sup>4+</sup> cations were successfully incorporated into the brucite-like layers of catalysts precursors. The presence of the promoters was found to strongly determine both the activity and the selectivity of these catalysts. The characterization of the spent catalysts showed that Ce addition led to the formation of higher amount of carbon deposits with respect to the non-promoted catalysts. However, the type of carbon deposits formed depended on the promoter used, and lower amounts of undesired graphitic carbon were observed over Ce-promoted samples in comparison to non-promoted catalyst. Moreover, Ce-promoted samples showed lower activity towards direct methane decomposition. Zirconia addition further inhibited this important side reaction, favouring the interaction of methane with CO<sub>2</sub> together with other important parallel reactions, such as reverse Boudouard reaction. Though lower conversions of both methane and CO<sub>2</sub> were measured for Zr-containing samples, almost no carbon was deposited on the catalysts surface upon 5 h of DRM reaction at 550 °C (Figure 5C). Carbon nanotubes were formed upon direct methane decomposition on Ni-containing catalysts.

The physicochemical characterization of the catalysts showed the formation of narrower porosity, resulting in higher surface areas for Zr-promoted catalysts. The XRD and TEM measurements confirmed the formation of small Ni crystallites (around 4 nm) in these two catalysts, which were considerably smaller than for the non-promoted sample (around 12 nm). Due to the active site size-selective character of the different reactions involved in DRM, such small Ni crystallites were not active in direct methane decomposition and favoured other side reactions, i.e., reverse Boudouard reaction. Moreover, the presence of Zr was found to promote the adsorption of CO<sub>2</sub> on weak and moderate strength basic sites, resulting in a favoured interaction of adsorbed CO<sub>2</sub> with methane, and thus enhancing selectivity towards DRM. There is no doubt that the very beneficial effect is connected to the synergetic effect between Zr and Ni species present in HT brucite-like layers. Zr promotion seems to be the guarantee of a stable DRM HT-derived catalyst. However, further research in this area is still needed.

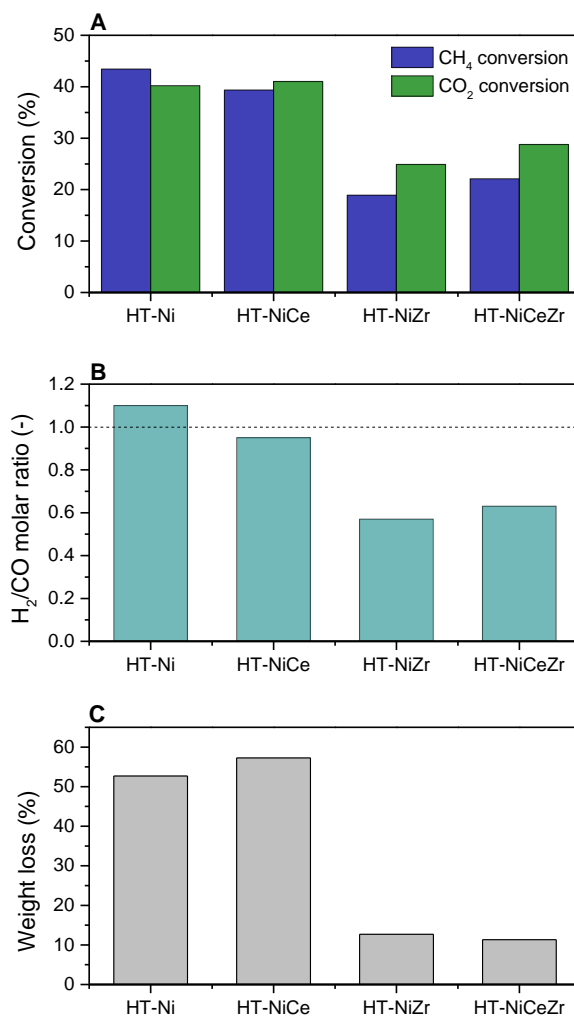


**Figure 5.** The results of DRM catalytic tests over Ce- and/or Zr-promoted catalysts: (A) CH<sub>4</sub> and CO<sub>2</sub> conversion (B) product distribution and (C) results of thermogravimetric measurements for spent catalysts. Adapted from [89].

#### 4. Conclusions

The present review aims to contain an overview of the recent advances in the use of nickel-containing hydrotalcite-derived catalysts for dry reforming of methane (DRM). The reviewed literature evidences that the catalytic activity, selectivity and stability of such materials is dependent on various factors including: the content of nickel in brucite-like layers, the method of nickel incorporation, the molar ratios of Ni/Mg, Ni/Al and M<sup>2+</sup>/M<sup>3+</sup> and the use of different promoters. Moreover, the catalytic behaviour strongly depends on the conditions chosen for the calcination and reduction pre-treatment of the catalysts. In general, hydrotalcite-derived catalysts showed high activity and adequate stability at relatively high temperatures, i.e., above 700 °C. However, the formation of carbonaceous deposits was still commonly observed. The extent of carbon formation, coking of the catalyst surface and deactivation depend on the physicochemical features of the catalyst. No general agreement can be found in the literature, about the key properties warranting a good catalytic stability. However, it is generally believed that Ni sintering and/or the presence of bigger Ni particle/crystals enhance direct methane decomposition, resulting in carbon formation. Some works remark that the carbon deposited can be easily removed via oxidation or hydrogasification. A further evaluation of the consequences of these regeneration thermal treatments on the state and properties of the Ni phase is needed. The incensement of material stability in low temperature DRM seems to be the most



challenging aspect, as low temperature DRM might be powered by non-emitting energy sources, such as renewables or small nuclear reactors. The proposed solutions in the literature include the use of different promoters, such as Ce, La, Zr, as well as other metals, such as Co and Mo. The presence of these promoters increase nickel-support interactions, preventing in this way sintering of nickel species and inhibiting C-forming side reactions. Very promising results were obtained for hydrotalcite-derived catalysts containing Zr species in the brucite-like layers. Further research is, however, essential in order to obtain stable and active catalysts, which will enable commercialization of the DRM process for chemical valorization of CO<sub>2</sub>.

**Acknowledgments:** R. Debek would like to acknowledge the French Embassy for financial support for his PhD in cotutelle between AGH and UPMC.

**Author Contributions:** All the authors contributed in summarizing all the data, writing and correcting this review.

**Conflicts of Interest:** The authors declare no conflict of interest.

## References

1. BP. Energy charting tool. British Petroleum BP plc. Available online: <http://tools.bp.com/energy-charting-tool> (accessed on 2 January 2016).
2. Lavoie, J.-M. Review on dry reforming of methane, a potentially more environmentally-friendly approach to the increasing natural gas exploitation. *Front. Chem.* **2014**, *2*. [[CrossRef](#)] [[PubMed](#)]
3. U.S. Energy Information Administration. International Energy Statistics. Available online: <http://www.eia.gov/cfapps/ipdbproject/IEDIndex3.cfm> (accessed on 6 January 2016).
4. United Nations Framework Convention on Climate Change. Kyoto Protocol. Available online: [http://unfccc.int/kyoto\\_protocol/items/2830.php](http://unfccc.int/kyoto_protocol/items/2830.php) (accessed on 1 September 2016).
5. United Nations Conference on Climate Change (COP21). Available online: <http://www.cop21.gouv.fr/en/> (accessed on 1 September 2016).
6. COM(2014) 15 Final, *Communication From The Commission To The European Parliament, The Council, The European Economic and Social Committee and The Committee of the Regions, A Policy Framework for Climate and Energy in the Period from 2020 to 2030*; European Commission: Brussels, Belgium, 2014; pp. 1–18.
7. European Commission. *Energy Roadmap 2050*; Publications Office of the European Union: Luxembourg, Belgium, 2012.
8. Bradford, M.C.J.; Vannice, M.A. CO<sub>2</sub> Reforming of CH<sub>4</sub>. *Catal. Rev.* **1999**, *41*, 1–42. [[CrossRef](#)]
9. Suhartanto, T.; York, A.P.E.; Hanif, A.; Al-Megren, H.; Green, M.L.H. Potential utilisation of Indonesia's Natuna natural gas field via methane dry reforming to synthesis gas. *Catal. Lett.* **2001**, *71*, 49–54. [[CrossRef](#)]
10. Richardson, J.T.; Paripatyadar, S.A. Carbon dioxide reforming of methane with supported rhodium. *Appl. Catal.* **1990**, *61*, 293–309. [[CrossRef](#)]
11. McCrary, J.H.; McCrary, G.E.; Chubb, T.A.; Nemecek, J.J.; Simmons, D.E. An experimental study of the CO<sub>2</sub> CH<sub>4</sub> reforming-methanation cycle as a mechanism for converting and transporting solar energy. *Sol. Energy* **1982**, *29*, 141–151. [[CrossRef](#)]
12. Chubb, T.A. Characteristics of CO<sub>2</sub>-CH<sub>4</sub> reforming-methanation cycle relevant to the solchem thermochemical power system. *Solar Energy* **1980**, *24*, 341–345. [[CrossRef](#)]
13. Mortensen, P.M.; Dybkjær, I. Industrial scale experience on steam reforming of CO<sub>2</sub>-rich gas. *Appl. Catal. A Gen.* **2015**, *495*, 141–151. [[CrossRef](#)]
14. Teuner, C.; Neumann, P.; Von Linde, F. The Calcor Standard and Calcor Economy Processes. *Oil Gas Eur. Mag.* **2001**, *3*, 44–46.
15. Reitmeier, R.E.; Atwood, K.; Bennett, H.; Baugh, H. Production of Synthetic Gas—Reaction of Light Hydrocarbons with Steam and Carbon Dioxide. *Ind. Eng. Chem.* **1948**, *40*, 620–626. [[CrossRef](#)]
16. Więclaw-Solny, L.; Łabojko, G.; Babiński, P. Możliwości przemysłowego wykorzystania ditlenku węgla—badania nad zastosowaniem CO<sub>2</sub> w procesie otrzymywania gazu syntezowego. *Polit. Energ.* **2009**, *12*, 633–642.
17. Rostrup-Nielsen, J. 40 years in catalysis. *Catal. Today* **2006**, *111*, 4–11.
18. Yun Hang, H. Advances in Catalysts for CO<sub>2</sub> Reforming of Methane. In *Advances in CO<sub>2</sub> Conversion and Utilization*; American Chemical Society: Washington, DC, USA, 2010; pp. 155–174.

19. Hei, M.J.; Chen, H.B.; Yi, J.; Lin, Y.J.; Lin, Y.Z.; Wei, G.; Liao, D.W. CO<sub>2</sub>-reforming of methane on transition metal surfaces. *Surf. Sci.* **1998**, *417*, 82–96. [[CrossRef](#)]
20. Kroll, V.C.H.; Swaan, H.M.; Mirodatos, C. Methane Reforming Reaction with Carbon Dioxide Over Ni/SiO<sub>2</sub> Catalyst: I. Deactivation Studies. *J. Catal.* **1996**, *161*, 409–422. [[CrossRef](#)]
21. Hu, Y.H.; Ruckenstein, E. *Catalytic Conversion of Methane to Synthesis Gas by Partial Oxidation and CO<sub>2</sub> Reforming*. *Advances in Catalysis*; Academic Press: Washington, DC, USA, 2004; pp. 297–345.
22. Ay, H.; Üner, D. Dry reforming of methane over CeO<sub>2</sub> supported Ni, Co and Ni–Co catalysts. *Appl. Catal. B Environ.* **2015**, *179*, 128–138. [[CrossRef](#)]
23. Becerra, A.; Dimitrijewits, M.; Arciprete, C.; Castro Luna, A. Stable Ni/Al<sub>2</sub>O<sub>3</sub> catalysts for methane dry reforming. *Granul. Matter* **2001**, *3*, 79–81. [[CrossRef](#)]
24. Kim, J.-H.; Suh, D.J.; Park, T.-J.; Kim, K.-L. Effect of metal particle size on coking during CO<sub>2</sub> reforming of CH<sub>4</sub> over Ni–alumina aerogel catalysts. *Appl. Catal. A Gen.* **2000**, *197*, 191–200. [[CrossRef](#)]
25. Li, L.; Zhang, L.-M.; Zhang, Y.-H.; Li, J.-L. Effect of Ni loadings on the catalytic properties of Ni/MgO(111) catalyst for the reforming of methane with carbon dioxide. *J. Fuel Chem. Technol.* **2015**, *43*, 315–322. [[CrossRef](#)]
26. Jafarbegloo, M.; Tarlani, A.; Mesbah, A.W.; Sahebdehfar, S. One-pot synthesis of NiO–MgO nanocatalysts for CO<sub>2</sub> reforming of methane: The influence of active metal content on catalytic performance. *J. Nat. Gas Sci. Eng.* **2015**, *27*, 1165–1173. [[CrossRef](#)]
27. Odedairo, T.; Chen, J.; Zhu, Z. Metal–support interface of a novel Ni–CeO<sub>2</sub> catalyst for dry reforming of methane. *Catal. Commun.* **2013**, *31*, 25–31. [[CrossRef](#)]
28. Pompeo, F.; Nichio, N.N.; Ferretti, O.A.; Resasco, D. Study of Ni catalysts on different supports to obtain synthesis gas. *Int. J. Hydrog. Energ.* **2005**, *30*, 1399–1405. [[CrossRef](#)]
29. Kroll, V.C.H.; Swaan, H.M.; Lacombe, S.; Mirodatos, C. Methane Reforming Reaction with Carbon Dioxide over Ni/SiO<sub>2</sub> Catalyst: II. A Mechanistic Study. *J. Catal.* **1996**, *164*, 387–398. [[CrossRef](#)]
30. Gálvez, M.E.; Albarazi, A.; Da Costa, P. Enhanced catalytic stability through non-conventional synthesis of Ni/SBA-15 for methane dry reforming at low temperatures. *Appl. Catal. A Gen.* **2015**, *504*, 143–150. [[CrossRef](#)]
31. Zhang, Z.; Verykios, X.E. Carbon dioxide reforming of methane to synthesis gas over Ni/La<sub>2</sub>O<sub>3</sub> catalysts. *Appl. Catal. A Gen.* **1996**, *138*, 109–133. [[CrossRef](#)]
32. Kim, S.S.; Lee, S.M.; Won, J.M.; Yang, H.J.; Hong, S.C. Effect of Ce/Ti ratio on the catalytic activity and stability of Ni/CeO<sub>2</sub>–TiO<sub>2</sub> catalyst for dry reforming of methane. *Chem. Eng. J.* **2015**, *280*, 433–440. [[CrossRef](#)]
33. Min, J.-E.; Lee, Y.-J.; Park, H.-G.; Zhang, C.; Jun, K.-W. Carbon dioxide reforming of methane on Ni–MgO–Al<sub>2</sub>O<sub>3</sub> catalysts prepared by sol–gel method: Effects of Mg/Al ratios. *J. Ind. Eng. Chem.* **2015**, *26*, 375–383. [[CrossRef](#)]
34. Alipour, Z.; Rezaei, M.; Meshkani, F. Effect of Ni loadings on the activity and coke formation of MgO-modified Ni/Al<sub>2</sub>O<sub>3</sub> nanocatalyst in dry reforming of methane. *J. Energy Chem.* **2014**, *23*, 633–638. [[CrossRef](#)]
35. Xu, L.; Song, H.; Chou, L. Ordered mesoporous MgO–Al<sub>2</sub>O<sub>3</sub> composite oxides supported Ni based catalysts for CO<sub>2</sub> reforming of CH<sub>4</sub>, Effects of basic modifier and mesopore structure. *Int. J. Hydrog. Energ.* **2013**, *38*, 7307–7325. [[CrossRef](#)]
36. Radlik, M.; Adamowska-Teyssier, M.; Krztoń, A.; Kozieł, K.; Krajewski, W.; Turek, W.; Da Costa, P. Dry reforming of methane over Ni/Ce<sub>0.62</sub>Zr<sub>0.38</sub>O<sub>2</sub> catalysts: Effect of Ni loading on the catalytic activity and on H<sub>2</sub>/CO production. *Comptes Rendus Chim.* **2015**, *18*, 1242–1249. [[CrossRef](#)]
37. Luisetto, I.; Tuti, S.; Battocchio, C.; Lo Mastro, S.; Sodo, A. Ni/CeO<sub>2</sub>–Al<sub>2</sub>O<sub>3</sub> catalysts for the dry reforming of methane: The effect of CeAlO<sub>3</sub> content and nickel crystallite size on catalytic activity and coke resistance. *Appl. Catal. A Gen.* **2015**, *500*, 12–22. [[CrossRef](#)]
38. Luengnaruemitchai, A.; Kaengsilalai, A. Activity of different zeolite-supported Ni catalysts for methane reforming with carbon dioxide. *Chem. Eng. J.* **2008**, *144*, 96–102. [[CrossRef](#)]
39. Nimwattanakul, W.; Luengnaruemitchai, A.; Jitkarnka, S. Potential of Ni supported on clinoptilolite catalysts for carbon dioxide reforming of methane. *Int. J. Hydrog. Energ.* **2006**, *31*, 93–100. [[CrossRef](#)]
40. Jabbour, K.; El Hassan, N.; Davidson, A.; Massiani, P.; Casale, S. Characterizations and performances of Ni/diatomite catalysts for dry reforming of methane. *Chem. Eng. J.* **2015**, *264*, 351–358. [[CrossRef](#)]
41. Liu, Y.; He, Z.; Zhou, L.; Hou, Z.; Eli, W. Simultaneous oxidative conversion and CO<sub>2</sub> reforming of methane to syngas over Ni/vermiculite catalysts. *Catal. Commun.* **2013**, *42*, 40–44. [[CrossRef](#)]

42. Daza, C.E.; Kiennemann, A.; Moreno, S.; Molina, R. Dry reforming of methane using Ni–Ce catalysts supported on a modified mineral clay. *Appl. Catal. A Gen.* **2009**, *364*, 65–74. [[CrossRef](#)]
43. Ma, Q.; Wang, D.; Wu, M.; Zhao, T.; Yoneyama, Y.; Tsubaki, N. Effect of catalytic site position: Nickel nanocatalyst selectively loaded inside or outside carbon nanotubes for methane dry reforming. *Fuel* **2013**, *108*, 430–438. [[CrossRef](#)]
44. Chen, Y.-G.; Ren, J. Conversion of methane and carbon dioxide into synthesis gas over alumina-supported nickel catalysts. Effect of Ni–Al<sub>2</sub>O<sub>3</sub> interactions. *Catal. Lett.* **1994**, *29*, 39–48. [[CrossRef](#)]
45. Bhattacharyya, A.; Chang, V.W. CO<sub>2</sub> Reforming of Methane to Syngas: Deactivation Behavior of Nickel Aluminate Spinel Catalysts. In *Studies in Surface Science and Catalysis*; Delmon, B., Froment, G.F., Eds.; Elsevier: Ostend, Belgium, 1994; pp. 207–213.
46. Baktash, E.; Littlewood, P.; Schomäcker, R.; Thomas, A.; Stair, P.C. Alumina coated nickel nanoparticles as a highly active catalyst for dry reforming of methane. *Appl. Catal. B Environ.* **2015**, *179*, 122–127. [[CrossRef](#)]
47. Zanganeh, R.; Rezaei, M.; Zamaniyan, A. Dry reforming of methane to synthesis gas on NiO–MgO nanocrystalline solid solution catalysts. *Int. J. Hydrog. Energ.* **2013**, *38*, 3012–3018. [[CrossRef](#)]
48. Zanganeh, R.; Rezaei, M.; Zamaniyan, A. Preparation of nanocrystalline NiO–MgO solid solution powders as catalyst for methane reforming with carbon dioxide: Effect of preparation conditions. *Adv. Powder Technol.* **2014**, *25*, 1111–1117. [[CrossRef](#)]
49. Cavani, F.; Trifirò, F.; Vaccari, A. Hydrotalcite-type anionic clays: Preparation, properties and applications. *Catal. Today* **1991**, *11*, 173–301. [[CrossRef](#)]
50. Forano, C.; Costantino, U.; Prévot, V.; Gueho, C.T. Chapter 14.1—Layered Double Hydroxides (LDH). In *Developments in Clay Science*; Faïza, B., Gerhard, L., Eds.; Elsevier: Amsterdam, The Netherlands, 2013; pp. 745–782.
51. Evans, D.G.; Slade, R.C.T. Structural Aspects of Layered Double Hydroxides. In *Layered Double Hydroxides*; Duan, X., Evans, D.G., Eds.; Springer: Berlin, Germany, 2006; pp. 1–87.
52. Rives, V.; Carriazo, D.; Martín, C. Heterogeneous Catalysis by Polyoxometalate-Intercalated Layered Double Hydroxides. In *Pillared Clays and Related Catalysts*; Gil, A., Korili, A.S., Trujillano, R., Vicente, A.M., Eds.; Springer: New York, NY, USA, 2010; pp. 319–397.
53. Zhu, Y.; Zhang, S.; Chen, B.; Zhang, Z.; Shi, C. Effect of Mg/Al ratio of NiMgAl mixed oxide catalyst derived from hydrotalcite for carbon dioxide reforming of methane. *Catal. Today* **2016**, *264*, 163–170. [[CrossRef](#)]
54. Perez-Lopez, O.W.; Senger, A.; Marcilio, N.R.; Lansarin, M.A. Effect of composition and thermal pretreatment on properties of Ni–Mg–Al catalysts for CO<sub>2</sub> reforming of methane. *Appl. Catal. A Gen.* **2006**, *303*, 234–244. [[CrossRef](#)]
55. Guo, J.; Lou, H.; Zhao, H.; Chai, D.; Zheng, X. Dry reforming of methane over nickel catalysts supported on magnesium aluminate spinels. *Appl. Catal. A Gen.* **2004**, *273*, 75–82. [[CrossRef](#)]
56. Gonzalez, A.R.; Asencios, Y.J.O.; Assaf, E.M.; Assaf, J.M. Dry reforming of methane on Ni–Mg–Al nano-spheroid oxide catalysts prepared by the sol-gel method from hydrotalcite-like precursors. *Appl. Surf. Sci.* **2013**, *280*, 876–887. [[CrossRef](#)]
57. Tsyganok, A.I.; Tsunoda, T.; Hamakawa, S.; Suzuki, K.; Takehira, K.; Hayakawa, T. Dry reforming of methane over catalysts derived from nickel-containing Mg–Al layered double hydroxides. *J. Catal.* **2003**, *213*, 191–203. [[CrossRef](#)]
58. Lin, X.; Li, R.; Lu, M.; Chen, C.; Li, D.; Zhan, Y.; Jiang, L. Carbon dioxide reforming of methane over Ni catalysts prepared from Ni–Mg–Al layered double hydroxides: Influence of Ni loadings. *Fuel* **2015**, *162*, 271–280. [[CrossRef](#)]
59. Daza, C.E.; Moreno, S.; Molina, R. Co-precipitated Ni–Mg–Al catalysts containing Ce for CO<sub>2</sub> reforming of methane. *Int. J. Hydrog. Energ.* **2011**, *36*, 3886–3894. [[CrossRef](#)]
60. Daza, C.E.; Cabrera, C.R.; Moreno, S.; Molina, R. Syngas production from CO<sub>2</sub> reforming of methane using Ce-doped Ni-catalysts obtained from hydrotalcites by reconstruction method. *Appl. Catal. A Gen.* **2010**, *378*, 125–133. [[CrossRef](#)]
61. Touahra, F.; Sehaïlia, M.; Ketir, W.; Bachari, K.; Chebout, R.; Trari, M.; Cherifi, O.; Halliche, D. Effect of the Ni/Al ratio of hydrotalcite-type catalysts on their performance in the methane dry reforming process. *Appl. Petrochem. Res.* **2016**, *6*, 1–13. [[CrossRef](#)]
62. Bhattacharyya, A.; Chang, V.W.; Schumacher, D.J. CO<sub>2</sub> reforming of methane to syngas: I: Evaluation of hydrotalcite clay-derived catalysts. *Appl. Clay Sci.* **1998**, *13*, 317–328. [[CrossRef](#)]

63. Basile, F.; Basini, L.; Amore, M.D.; Fornasari, G.; Guarinoni, A.; Matteuzzi, D.; Pieroc, G.D.; Trifirò, F.; Vaccaria, A. Ni/Mg/Al Anionic Clay Derived Catalysts for the Catalytic Partial Oxidation of Methane: Residence Time Dependence of the Reactivity Features. *J. Catal.* **1998**, *173*, 247–256. [[CrossRef](#)]
64. Dębek, R.; Motak, M.; Duraczyska, D.; Launay, F.; Galvez, M.E.; Grzybek, T.; Da Costa, P. Methane dry reforming over hydrotalcite-derived Ni-Mg-Al mixed oxides: The influence of Ni content on catalytic activity, selectivity and stability. *Catal. Sci. Technol.* **2016**, *6*, 6705–6715. [[CrossRef](#)]
65. Djebbari, B.; Gonzalez-Delacruz, V.M.; Halliche, D.; Bachari, K.; Saadi, A.; Caballero, A.; Holgado, J.; Cherifi, O. Promoting effect of Ce and Mg cations in Ni/Al catalysts prepared from hydrotalcites for the dry reforming of methane. *React. Kinet. Mech. Catal.* **2013**, *111*, 259–275. [[CrossRef](#)]
66. Dębek, R.; Zubek, K.; Motak, M.; Galvez, M.E.; Da Costa, P.; Grzybek, T. Ni–Al hydrotalcite-like material as the catalyst precursors for the dry reforming of methane at low temperature. *Comptes Rendus Chim.* **2015**, *18*, 1205–1210. [[CrossRef](#)]
67. Mette, K.; Kühl, S.; Düdder, H.; Kähler, K.; Tarasov, A.; Muhler, M.; Behrens, M. Stable Performance of Ni Catalysts in the Dry Reforming of Methane at High Temperatures for the Efficient Conversion of CO<sub>2</sub> into Syngas. *Chemcatchem* **2014**, *6*, 100–104. [[CrossRef](#)]
68. Mette, K.; Kühl, S.; Tarasov, A.; Düdder, H.; Kähler, K.; Muhler, M.; Schloegl, R.; Behrens, M. Redox dynamics of Ni catalysts in CO<sub>2</sub> reforming of methane. *Catal. Today* **2015**, *242*, 101–110. [[CrossRef](#)]
69. Abdelsadek, Z.; Sehailia, M.; Halliche, D.; Gonzalez-Delacruz, V.M.; Holgado, J.P.; Bachari, K.; Caballero, A.; Cherifi, O. In-situ hydrogasification/regeneration of NiAl-hydrotalcite derived catalyst in the reaction of CO<sub>2</sub> reforming of methane: A versatile approach to catalyst recycling. *J. CO<sub>2</sub> Util.* **2016**, *14*, 98–105. [[CrossRef](#)]
70. Dudder, H.; Kahler, K.; Krause, B.; Mette, K.; Kuhl, S.; Behrens, M.; Scherer, V.; Muhler, M. The role of carbonaceous deposits in the activity and stability of Ni-based catalysts applied in the dry reforming of methane. *Catal. Sci. Technol.* **2014**, *4*, 3317–3328. [[CrossRef](#)]
71. Shishido, T.; Sukenobu, M.; Morioka, H.; Furukawa, R.; Shirahase, H.; Takehira, K. CO<sub>2</sub> reforming of CH<sub>4</sub> over Ni/Mg–Al oxide catalysts prepared by solid phase crystallization method from Mg–Al hydrotalcite-like precursors. *Catal. Lett.* **2001**, *73*, 21–26. [[CrossRef](#)]
72. Tan, P.; Gao, Z.; Shen, C.; Du, Y.; Li, X.; Huang, W. Ni-Mg-Al solid basic layered double oxide catalysts prepared using surfactant-assisted coprecipitation method for CO<sub>2</sub> reforming of CH<sub>4</sub>. *Chin. J. Catal.* **2014**, *35*, 1955–1971. [[CrossRef](#)]
73. Tsyganok, A.I.; Suzuki, K.; Hamakawa, S.; Takehira, K.; Hayakawa, T. Mg–Al Layered Double Hydroxide Intercalated with [Ni(EDTA)]<sup>2-</sup> Chelate as a Precursor for an Efficient Catalyst of Methane Reforming with Carbon Dioxide. *Catal. Lett.* **2001**, *77*, 75–86. [[CrossRef](#)]
74. Dębek, R.; Zubek, K.; Motak, M.; Da Costa, P.; Grzybek, T. Effect of nickel incorporation into hydrotalcite-based catalyst systems for dry reforming of methane. *Res. Chem. Intermed.* **2015**, *41*, 9485–9495. [[CrossRef](#)]
75. Hou, Z.; Yashima, T. Meso-porous Ni/Mg/Al catalysts for methane reforming with CO<sub>2</sub>. *Appl. Catal. A Gen.* **2004**, *261*, 205–209. [[CrossRef](#)]
76. Li, N.; Shen, C.; Tan, P.; Zou, Z.; Huang, W. Effect of phase transformation on the stability of Ni-Mg-Al catalyst for dry reforming of methane. *Indian J. Chem.* **2015**, *54A*, 1198–1205.
77. Rives, V. Characterisation of layered double hydroxides and their decomposition products. *Mater. Chem. Phys.* **2002**, *75*, 19–25. [[CrossRef](#)]
78. Lwin, Y.; Yarmo, M.A.; Yaakob, Z.; Mohamad, A.B.; Ramli Wan Daud, W. Synthesis and characterization of Cu–Al layered double hydroxides. *Mater. Res. Bull.* **2001**, *36*, 193–198. [[CrossRef](#)]
79. Kannan, S.; Dubey, A.; Knozinger, H. Synthesis and characterization of CuMgAl ternary hydrotalcites as catalysts for the hydroxylation of phenol. *J. Catal.* **2005**, *231*, 381–392. [[CrossRef](#)]
80. Velu, S.; Suzuki, K.; Kapoor, M.P.; Tomura, S.; Ohashi, F.; Osaki, T. Effect of Sn Incorporation on the Thermal Transformation and Reducibility of M(II)Al-Layered Double Hydroxides [M(II) = Ni or Co]. *Chem. Mater.* **2000**, *12*, 719–730. [[CrossRef](#)]
81. Yu, M.; Zhu, Y.-A.; Lu, Y.; Tong, G.; Zhu, K.; Zhou, X. The promoting role of Ag in Ni-CeO<sub>2</sub> catalyzed CH<sub>4</sub>-CO<sub>2</sub> dry reforming reaction. *Appl. Catal. B Environ.* **2015**, *165*, 43–56. [[CrossRef](#)]
82. Daza, C.E.; Gallego, J.; Moreno, J.A.; Mondragón, F.; Moreno, S.; Molina, R. CO<sub>2</sub> reforming of methane over Ni/Mg/Al/Ce mixed oxides. *Catal. Today* **2008**, *133–135*, 357–366. [[CrossRef](#)]

83. Daza, C.E.; Gallego, J.; Mondragón, F.; Moreno, S.; Molina, R. High stability of Ce-promoted Ni/Mg–Al catalysts derived from hydrotalcites in dry reforming of methane. *Fuel* **2010**, *89*, 592–603. [[CrossRef](#)]
84. Daza, C.E.; Moreno, S.; Molina, R. Ce-incorporation in mixed oxides obtained by the self-combustion method for the preparation of high performance catalysts for the CO<sub>2</sub> reforming of methane. *Catal. Commun.* **2010**, *12*, 173–179. [[CrossRef](#)]
85. Lino, A.V.P.; Assaf, E.M.; Assaf, J.M. Hydrotalcites derived catalysts for syngas production from biogas reforming: Effect of nickel and cerium load. *Catal. Today* [[CrossRef](#)]
86. Ren, H.-P.; Song, Y.-H.; Wang, W.; Chen, J.-G.; Cheng, J.; Jiang, J.; Liu, Z.T.; Hao, Z.; Lu, J. Insights into CeO<sub>2</sub>-modified Ni–Mg–Al oxides for pressurized carbon dioxide reforming of methane. *Chem. Eng. J.* **2015**, *259*, 581–593. [[CrossRef](#)]
87. Dębek, R.; Radlik, M.; Motak, M.; Galvez, M.E.; Turek, W.; Da Costa, P.; Grzybek, T. Ni-containing Ce-promoted hydrotalcite derived materials as catalysts for methane reforming with carbon dioxide at low temperature—On the effect of basicity. *Catal. Today* **2015**, *257*, 59–65. [[CrossRef](#)]
88. Dębek, R.; Gramatyka, A.; Motak, M.; Da Costa, P. Produkcja gazu syntezowego w reakcji suchego reformingu metanu na katalizatorach hydrotalkitowych, Syngas production by dry reforming of methane over hydrotalcite-derived catalysts. *Przem. Chem.* **2014**, *93*, 2026–2032.
89. Dębek, R.; Galvez, M.E.; Launay, F.; Motak, M.; Grzybek, T.; Da Costa, P. Low temperature dry methane reforming over Ce, Zr and CeZr promoted Ni–Mg–Al hydrotalcite-derived catalysts. *Int. J. Hydrog. Energ.* **2016**, *41*, 11616–11623. [[CrossRef](#)]
90. Yu, X.; Wang, N.; Chu, W.; Liu, M. Carbon dioxide reforming of methane for syngas production over La-promoted NiMgAl catalysts derived from hydrotalcites. *Chem. Eng. J.* **2012**, *209*, 623–632. [[CrossRef](#)]
91. Serrano-Lotina, A.; Rodríguez, L.; Muñoz, G.; Martín, A.J.; Folgado, M.A.; Daza, L. Biogas reforming over La–NiMgAl catalysts derived from hydrotalcite-like structure: Influence of calcination temperature. *Catal. Commun.* **2011**, *12*, 961–967. [[CrossRef](#)]
92. Serrano-Lotina, A.; Rodríguez, L.; Muñoz, G.; Daza, L. Biogas reforming on La-promoted NiMgAl catalysts derived from hydrotalcite-like precursors. *J. Power Sources* **2011**, *196*, 4404–4410. [[CrossRef](#)]
93. Liu, H.; Wierzbicki, D.; Dębek, R.; Motak, M.; Grzybek, T.; Da Costa, P.; Galvez, M. La-promoted Ni-hydrotalcite-derived catalysts for dry reforming of methane at low temperatures. *Fuel* **2016**, *182*, 8–16. [[CrossRef](#)]
94. Lucrédio, A.F.; Assaf, J.M.; Assaf, E.M. Reforming of a model sulfur-free biogas on Ni catalysts supported on Mg(Al)O derived from hydrotalcite precursors: Effect of La and Rh addition. *Biomass Bioenergy* **2014**, *60*, 8–17. [[CrossRef](#)]
95. Li, C.; Tan, P.J.; Li, X.D.; Du, Y.L.; Gao, Z.H.; Huang, W. Effect of the addition of Ce and Zr on the structure and performances of Ni–Mo/CeZr–MgAl(O) catalysts for CH<sub>4</sub>–CO<sub>2</sub> reforming. *Fuel Process. Technol.* **2015**, *140*, 39–45. [[CrossRef](#)]
96. Tsyganok, A.I.; Inaba, M.; Tsunoda, T.; Uchida, K.; Suzuki, K.; Takehira, K.; Hayakawa, T. Rational design of Mg–Al mixed oxide-supported bimetallic catalysts for dry reforming of methane. *Appl. Catal. A Gen.* **2005**, *292*, 328–343. [[CrossRef](#)]
97. Long, H.; Xu, Y.; Zhang, X.; Hu, S.; Shang, S.; Yin, Y.; Dai, X. Ni–Co/Mg–Al catalyst derived from hydrotalcite-like compound prepared by plasma for dry reforming of methane. *J. Energy Chem.* **2013**, *22*, 733–739. [[CrossRef](#)]
98. Zhang, J.; Wang, H.; Dalai, A.K. Effects of metal content on activity and stability of Ni–Co bimetallic catalysts for CO<sub>2</sub> reforming of CH<sub>4</sub>. *Appl. Catal. A Gen.* **2008**, *339*, 121–129. [[CrossRef](#)]

